Economics of Residential Photovoltaic and Wind Systems in Arizona and California

by

Wen An

A Thesis Presented in Partial Fulfillment
of the Requirements for the Degree
Master of Science

Approved July 2012 by the
Graduate Supervisory Committee:

Keith Holbert, Chair
George Karady
Daniel Tylavsky

ARIZONA STATE UNIVERSITY

August 2012

ABSTRACT

Renewable energy has been a very hot topic in recent years due to the traditional energy crisis. Incentives that encourage the renewables have been established all over the world. Ordinary homeowners are also seeking ways to exploit renewable energy. In this thesis, residential PV system, wind turbine system and a hybrid wind/solar system are all investigated.

The solar energy received by the PV panels varies with many factors. The most essential one is the irradiance. As the PV panel been installed towards different orientations, the incident insolation received by the panel also will be different. The differing insolation corresponds to the different angles between the irradiance and the panel throughout the day. The result shows that for PV panels in the northern hemisphere, the ones facing south obtain the highest level insolation and thus generate the most electricity. However, with the two different electricity rate plans, flat rate plan and TOU (time of use) plan, the value of electricity that PV generates is different.

For wind energy, the wind speed is the most significant variable to determine the generation of a wind turbine. Unlike solar energy, wind energy is much more regionally dependent. Wind resources vary between very close locations. As expected, the result shows that, larger wind speed leads to more electricity generation and thus shorter payback period.

For the PV/wind hybrid system, two real cases are analyzed for Altamont and Midhill, CA. In this part, the impact of incentives, system cost and system size are considered. With a hybrid system, homeowners may choose different size combinations between PV and wind turbines. It turns out that for these two locations, the system with larger PV output always achieve a shorter payback period due to the lower cost. Even though, for a longer term, the system with a larger wind turbine in locations with excellent wind resources may lead to higher return on investment. Meanwhile, impacts of both wind and solar incentives (mainly utility rebates) are analyzed. At last, effects of the cost of both renewables are performed.

TABLE OF CONTENTS

Page

CHAPTER

CHAPTER Page

CHAPTER Page

LIST OF TABLES

Table Page

LIST OF FIGURES

Figure Page

1. INTRODUCTION

This chapter addresses the motivation behind this research topic and also the objective.

1.1 Motivation and Background Review

Most countries of the world have encountered a shortage of energy supply, which cannot satisfy the need of economic development. Coal, oil and other fossil energy use produces large amounts of greenhouse gases, and pollute the environment. These problems have led to a global boom in renewable energy. Energy strategy established all over the world indicates that large-scale development and utilization of renewable energy has become the trend in the future.

During the period from the end of 2005 through 2010, total global capacity of many renewable energy technologies grew at average rates ranging from around 15% [1] to nearly 50% annually. Photovoltaic (PV) increased the fastest of all renewables technologies during this period, followed by biodiesel and wind.

It is essential that solar energy and renewable energy sources are increasingly used as a part of the world’s strategy to improve the security of energy supplies and reduce the impact of energy production and consumption. And photovoltaic (PV) insolation-harnessing is acknowledged as one of the most practical economic solutions to meet the requirements. Thus, in recent years, the photovoltaic market expanded extensively, especially in Germany, followed by Japan, Spain and the U.S.

In 1990, Germany began to carry out the "1000 Roof Program", and ended with 2500 photovoltaic systems installed on residential roofs. Furthermore, in 1999, the new “100000 Solar Roof Program” was carried out in Germany and in 2004, a new incentive policy was implemented to allow different acquisition price for PV power, which led to a boom in PV systems installation. Japan has a long history promoting residential photovoltaic systems. In 1994, they started to implement the "Seventy thousand Roof" program with a maximum subsidy of $7.5/W (up to 50% of installed costs) per system, which has declined to $1/W (up to 33% of installed costs) in 2001. Approximately, 300 MW of PV was installed under the program.

In the United States, the PV market is primarily encouraged by the government. From the Database of State Incentives for Renewables and Efficiency (DSIRE), 38 states have implemented the Renewables Portfolio Standards (RPS). Most of the states also have set up all kinds of incentive policies to encourage PV installation. As a result, the installation size of PV has increased significantly in recent years as shown in Figure 1.

Meanwhile, wind has had a dramatic increase during 2001 to 2010, specifically 1488% increase or 37.2% per year increase by 2009 as seen in Table 1 and Figure 2. And the U.S. has abundant wind resource and a favorable political environment. As shown in reference [2], the potential wind energy in the U.S. is huge; various regions have a tremendous availability of wind.

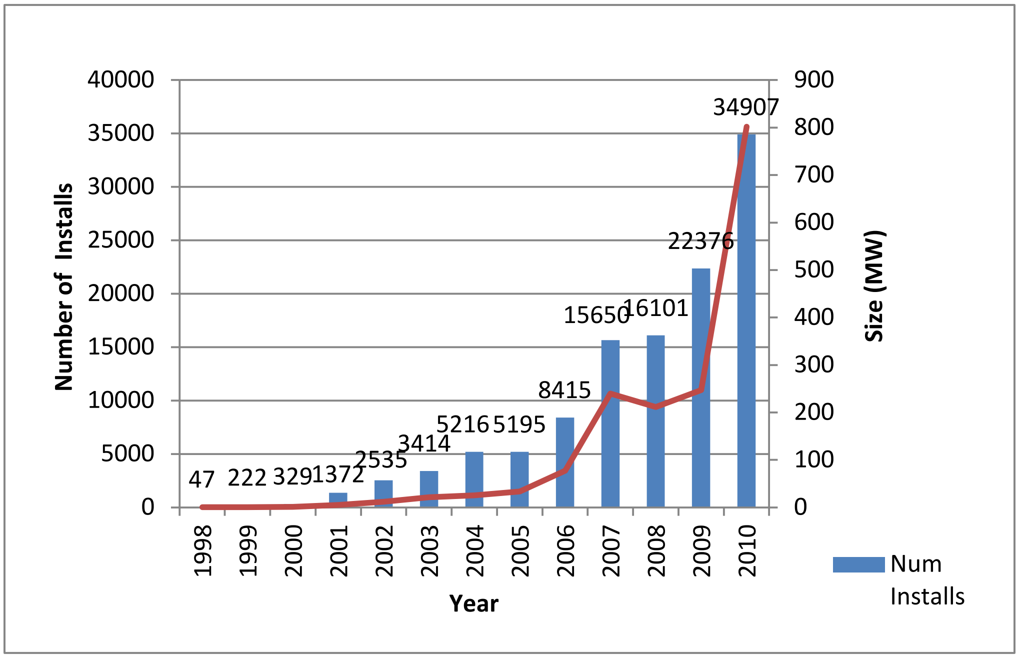

Figure 1 Installs and size of PV by year for U.S.; data from [1].

Table 1: Installs and size of wind generation by year for the U.S.

Year	U.S. Total (MW)	Increase (MW)	Increase (%)
2000	2,539	67	2.7%
2001	4,232	1,693	66.7%
2002	4,687	455	10.7%
2003	6,350	1,663	35.4%
2004	6,723	373	5.8%
2005	9,147	2,424	36.0%
2006	11,575	2,428	26.5%
2007	16,907	5,332	46.0%
2008	25,410	8,503	50.2%
2009	34,863	9,453	37.2%
2010	40,180	5,317	15.2%
2011(3Q)	43,461	3,360	8.1%

Source: Office of Energy Efficiency and Renewable Energy [3]

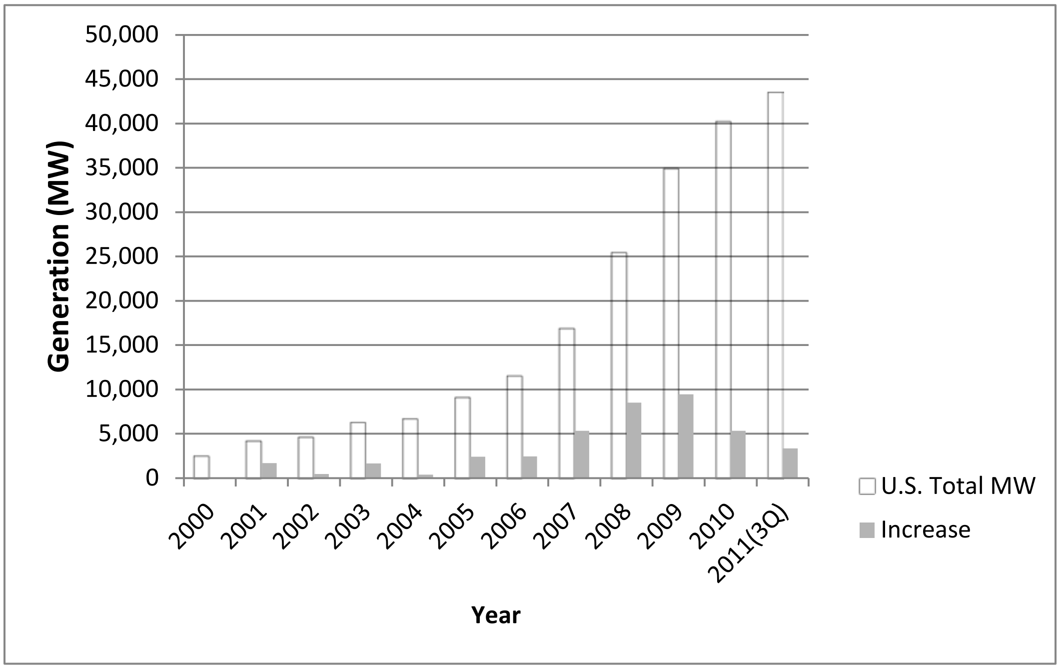

Figure 2 Wind electric energy capacity growth in the U.S.; data from [3]

1.2 Objective

According to [4], as of 2009, energy consumption of solar thermal/PV and wind power is only 0.819 quadrillion Btu which only made up 10% of the total renewable energy consumption in the U.S. That is far from the federal or state target.

PV systems face several barriers, in which the inevitable major one is the cost. Hence, analysis of the cost of residential sized PV system and wind turbine systems is necessary. However, the cost of renewable energy systems varies from state to state due to the different environment parameters, electricity rate plans and also the different policies and incentives. In this thesis, the environmental variables and specific policies will be taken into account, and reasonable economic suggestions will be given with simulations and calculations. Apart from that, the detailed cost of each component will be listed; profitability and earning cycle will also be illustrated.

In PV systems the operating temperature plays a important role in the PV system performance. The output power of a PV panel decreases with T_c, the PV cell temperature, which is a function of weather variables such as the ambient temperature, T_a, wind speed V_w, and solar irradiance I_r, as well as some material parameters. On the other hand, the irradiance is also the most important factor determining the output power. The temperature model equation used is shown as following [5],

$$T_c = 0.02 * I_r + T_a \tag{1}$$

Where T_c is the PV cell temperature (℃); T_a is the ambient temperature (℃); I_r is the solar irradiance (W/m^2);

And for wind models, wind speed is always the central factor that determines the system generation.

Obviously, series of long-term environmental data are needed to calculate the output of a PV array and a wind turbine. Hourly data of solar direct irradiance, ambient temperature and wind speed are available for more than one year from the Measurement and Instrumentation Data Center (MIDC), which belongs to the NREL (National Renewable Energy Laboratory). And data for multiple locations will be chosen to illustrate the influence and relations between each variable and the result. MATLAB will be used to rearrange and modify the ASCII data into usable ones.

Besides, incentives and polices for each chosen location are also essential for the calculation. Incentives including federal and state tax credits, cash incentives provided by the state and utility, net metering, etc, which can be obtained from the DSIRE, will be fully considered. Residential Power Purchase Agreement (PPA) rate plans are excluded in this work.

With the all the data above, the model for the PV arrays becomes possible. This effort will establish a MATLAB program to simulate the performance of the solar panel and Newton type iterative method will be applied to solve the maximum outputs of the PV panel. Furthermore, with the electrical plan and incentive data we can establish the cost model for a given residential home.

1.3 Solar Energy Characteristics

The solar energy is widely recommended as the following advantages,

1) Solar energy is theoretically inexhaustible, with an energy exposure to earth which is 6000 [6] times the energy consumed by humans.
2) Solar energy is widely and closely available. We can easily obtain locally instead of shipping power through long transmission lines which is more economic and also avoids the line loss.
3) Solar power generation does not need a 24 hour human guard. Thus, it is more convenient to maintain for ordinary customers.
4) A solar system is easy to build based on the mature module production these days.

5) Furthermore, solar energy is really clean energy without pollution. It does not produce any trash nor noise pollution.

While the solar energy also has some disadvantages:

1) Radiance to the ground is intermittent; generating capacity is related to the climate. In the evenings or cloudy days there will be no power generation or very little power generation, which will not satisfy the power that the loads need. Thus PV systems are usually equipped with an energy storage device.
2) Energy density is low, which means large areas of land are required to obtain significant power generation.
3) Even the cost for a residential sized PV system has declined significantly in recent years, but compared to the other traditional energy source, it still requires a higher initial investment.

1.4 Wind Energy Characteristics

Wind energy is abundant and wind turbine technology is mature. However, due to the stochastic characteristic of wind energy, wind power is an intermittent source. The output of wind power is random and mainly depends on the wind speed which is a random and uncontrollable variable. In addition, factors, such as wind turbulence and wake effects of wind turbines, can also cause turbulence that may result in the fluctuations of wind power and frequent starting and stoping of wind turbines. Also, because of the tower shadowing effect of the wind turbine, there is a cyclical fluctuation in the output power. Wind farms are mostly located remotely from the main power system and the load center. Wind power, as an unstable energy source due to the former reasons, will cause some impact on the grid and transmission system. So they should be carefully planned and modeled.

1.5 Literature review

Previous work has have been done in this field. In [7], breakeven costs are examined for residential PV with investigation of 1000 utilities in the U.S. during the period of late 2008 to early 2009. In this paper, the author emphasized the impacts of electricity cost, the rate plan and availability of the incentives, regardless of the impacts of solar energy resources and orientations. It was found that the breakeven conditions tend to appear first in Southwest where there are abundant energy resources, and then in the Northeast where there are high electricity prices. Also, in [8] the cost of residential PV was investigated based on three specific locations: Sacramento, California; Boulder, Colorado; and Newark, New Jersey. Various incentives are examined, including mortgage loans, federal, state and utility incentives, third-party ownership models and property tax assessment model. Then the traditional financing was compared. Meanwhile, [9] illustrates a special view of the PV system, specifically the effects of a PV system on the home prices in California is discussed. The report shows that homes with PV systems in California are sold prior to comparable ones without PV systems. On the other hand, wind systems are also analyzed. Report [10] explored the small wind turbines by reviewing the world’s wind turbine manufacturers and the utility grid-tied small wind turbine applications by 2000. Three specific turbines were chosen and tested in California, Minnesota, and South Dakota. And it turned out that California led to the shortest payback period because of the best incentives and high retail electricity rate. While [11] describes the economic wind turbine selection based on the assessment of the wind turbine operation stability and reliability. Wind turbines with higher rating power may have the lower economic efficiency due to the poor operation stability, and higher operation and maintenance costs. Then PV/wind hybrid system is discussed in [12] and [13]. A solar wind hybrid system in India is presented in [12]. Then simulations are applied to optimize the initial cost and optimum utilization of the resources. In [13], a real life example in western Maryland was provided to estimate the performance of a PV-wind system in surrounding region. It can be concluded that the experiment location does not have adequate wind resources for wind generation.

1.6 Outline of the Thesis

PV and wind systems are investigated separately in Chapter 2 and Chapter 3, respectively. Then the PV/wind hybrid system is presented in Chapter 4. Chapter 2 begins with a model of PV system. Then the cost of PV is analyzed, including the PV panel cost, the equipment cost and the labor cost. Apart from that, the incentives are considered which can reduce the cost. Federal tax credit, state tax credit, utility rebate and net metering are included. With the net metering, the performance of PV varies depending on the orientation installed. Thus, PV performance based on different orientations is illustrated subsequently. In Chapter 3, classification of wind turbines based on capacity size is introduced first. Then, two specific grid-tied small wind turbines which are applicable for residential use are presented. Furthermore, the modeling of wind turbines is processed. Thus the cost of wind turbines can be calculated accordingly with the incentives applied. Payback condition is given next. At last, the PV and wind are combined as a hybrid system. With the model of PV and wind system in previous chapters, the generation of the hybrid system can be modeled. Two locations in California are chosen to research the economic performance of a hybrid system under different circumstances including different PV-wind size combination, different incentive value and different system cost.

2. SOLAR PV

A PV array is an essential part of a residential solar energy system. Its I-V characteristic is a nonlinear function of the sun radiation intensity, temperature and PV module parameters. In practical applications, PV modules are usually connected in series or parallel, and assembled into a M × N photovoltaic array (M, N respectively for quantity of photovoltaic module series and parallels). To realize the simulation of the solar energy system, the first step is to simulate the I-V characteristics of a PV array.

2.1 Mathematical Model of PV Array

The mathematical model used in this thesis is as follows:

First, an equivalent circuit of a PV cell is shown in Figure 3.

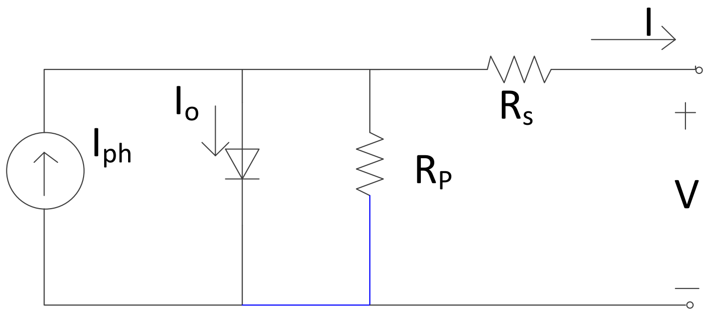

Figure 3 Equivalent circuit of a PV cell [14].

The equivalent equation can be expressed as follows,

$$I = I_{ph} - I_0 (\exp\left(\frac{V + R_s I}{V_t a}\right) - 1) - \frac{V + R_s I}{R_p} \tag{2}$$

Where,

I_{ph}: the solar-generated current;

I_o : the diode saturation current;

V_t: equals $N_s kT/q$, the thermal voltage of the array;

q: the electron charge, equals 1.602 10^{-19} C;

k: the Boltzmann constant, equals 1.380 10^{-23} J/K;

a: the diode ideality constant;

R_s: series resistance;

R_p: parallel resistance.

The solar-generated current, I_{ph} linearly depends on solar irradiance and influenced by temperature based on (3) [14].

$$I_{ph} = \frac{G}{G_n}[I_{ph,n} + K_i(T - T_n)] \tag{3}$$

Where,

$I_{ph,n}$: the solar generated current at the nominal condition (25 $°C$ and 1 kW/m^2);

G: the irradiance;

G_n: the nominal irradiance;

T: the cell temperature;

T_n: is the nominal cell temperature;

K_i: is the short-circuit current/temperature coefficient.

The diode saturation current, I_0 which depends on temperature is given by (4) [11].

$$I_0 = I_{o,n}\left(\frac{T}{T_n}\right)\exp\left[\frac{qE_g}{ak}\left(\frac{1}{T_n}-\frac{1}{T}\right)\right] \tag{4}$$

Where:

$I_{o,n}$: the nominal diode saturation current;

E_g: the band gap energy, equals 1.12 eV.

The nominal diode saturation current, $I_{o,n}$ can be expressed by (5) [13].

$$I_{o,n} = \frac{I_{sc,n}}{\left[\exp\left(\frac{V_{oc,n}}{aV_{t,n}}\right)\right]-1} \tag{5}$$

Where:

$V_{oc,n}$: the nominal open-circuit voltage;

$V_{t,n}$: the nominal thermal voltage of the cell;

$I_{sc,n}$: the short-circuit current at the nominal condition (25 °C and 1 kW/m^2).

A practical PV array consists of several connected PV modules formed by N_s solar cells connected in series and N_p in parallel. Therefore, (2) which presents a single PV cell should be amended into (6) to represent a PV array [11],

$$I = N_p I_{pv} - N_p I_o\left[\exp\left(\frac{V + I\cdot R_s\left(\frac{N_S}{N_p}\right)}{V_t a N_S}\right)-1\right] - \frac{V + I\cdot R_S\left(\frac{N_S}{N_p}\right)}{R_P\left(\frac{N_S}{N_p}\right)} \tag{6}$$

Most of the parameters in the presented equations can be obtained from datasheet provided by the manufacturer, an example of which is shown in Table 2.

Table 2: Specifications of SunTech Power-190W Solar Panel

Open circuit voltage (V_{oc})	45.5 V
Short circuit current (I_{sc})	5.69 A
Maximum power voltage (V_{mp})	36.6 V
Maximum power current (I_{mp})	5.33 A
Maximum power (P_{max})	195 W
Temperature coefficient of I_{sc} (K_i)	0.037 %/ °C
Temperature coefficient of V_{oc} (K_v)	-0.34 %/ °C

In this thesis, Maximum Power Point Tracking (MPPT) is assumed to be applied in the model, thus a MATLAB program is developed to calculate the output of a PV system based on the algorithm. The process is shown in the flowchart as Figure 4.

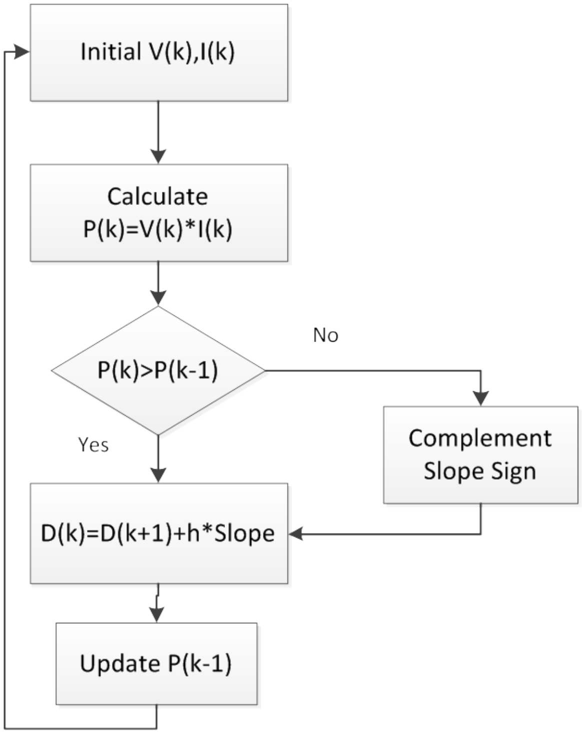

Figure 4 Power output calculating algorithm flowchart.

2.2 Cost of PV

The system initial cost is determined by the market, including the installation cost and labor cost. While during the operation, there will also be maintenance and operation cost. However, with the incentives by the federal, state and utility, those costs can also be reduced by some extent.

2.2.1 Initial Cost

An example is given as follows: here we presume that a homeowner in Arizona is purchasing a 4 kW grid-tied PV system that will be mounted on the roof of their home. According to Affordable-solar.com, we use a SunTech Power, 190 W Solar Panel, which is the world's largest solar panel manufacturer. With 21 panels rated at 190 watts, this system should generate a total theoretical output of 3,990 watts. According to Affordable-solar.com, we use a SunTech Power, 190 W Solar Panel, which is the world's largest solar panel manufacturer. With 21 panels rated at 190 watts, this system should generate a total theoretical output of 3,990 watts. Table 3 shows the components that will make up the system and the costs.

Table 3 Components of the 4 kW PV system cost

	Quantity	Cost per unit	Total cost
SunTech Power, 190W Solar Panel	21	$256.5	$5386.5
PVPowered 4000 watt inverter	1	$2,104	$2,104
Tyco Cable assembly and cable gland	1	$65	$65
Delta DC lightning arrestor	1	$40	$40
Delta AC lightning arrestor	1	$42	$42
UniRac Standard Rail Flush Mount	3	$300	$900
SubTotal for Equipment			$8537.5
Sales Tax (estimated 9%)			$768
SubTotal for Equipment with tax			$9306
Labor	35	$120	$4,200
SubTotal			$13506

The inverter is also very critical for a PV system. With an inverter, the DC electricity generated from the PV panels is converted to the AC electricity which can supply to the house. Here we choose a 4 kW inverter to suit the PV system capacity. Wiring is also needed to wire the panels together and connect the panels to the inverter. The connectors that connect the panels to each other are attached with the panels. And the connection of strings to the junction box and then to the inverter is also necessary. In this case, the junction box comes with the solar panel provided by the manufacturer. According to The National Electric Code [15], all panels are required to be completely grounded. Thus, copper wires for grounding the panels are also needed.

Furthermore, panels are electrical components sitting on a roof. In case of lightning strikes, AC and DC lightning arrestors is equipped to provide a protection against damage from lightning strikes. Hence two Delta lightning arrestor are added.

Also to mount the panels on the roof, a UniRac solar panel rail kit is applied. The rail kit is sized based on the assumption that the PV panels will be mounted on the roof with three racks each holding 7 panels. The panels will be mounted in a fixed orientation based upon the latitude to optimize the energy output.

Meanwhile, in this case, we assume that the labor will be done by experienced pv installers and electrician. And we estimated that it takes about 35 hours [4] for the labor to set up the system. However, labor rates vary from location to location. Also the price may go higher if the roof combined with some unique site requirements. Here we assume an hourly rate of $120 per hour.

From Table 3 we can calculate that, in this case, the initial cost for a 3.99 kW sized grid-tied PV system is approximately $3.4/W.

2.2.2 Incentives

Figure 5 illustrates a grid-tied residential sized PV system. Generation from the PV panel can supply the customer house, and the excess part can be sent back to the utility. And with the net metering, the utility purchases the excess power at the avoided cost, or at the average retail rate. This reduces the monthly bill of the homeowner, or can be considered to reduce the system cost. Usually, net metering rules are determined by state basis, sometimes by the legislature or the Public Utilities Commission (PUC). APS provides two types of net metering rate plans ERP-2 and ERP-6. And the electricity saving amount can be calculated corresponding to those different electricity plans. Also there are also other incentives implemented in Arizona. Table 4 shows the applicable incentives in this case.

Table 4: Incentives specifics for PV with APS in Arizona

Federal Incentive Tax credit		30% of the initial cost
Utility (APS) Rebate Program		$ 0.6/W rebate with a cap of 10 kW
Net metering	ERP-2	$ 0.1/W
	ERP-3	TOU price

Thus the remaining cost of a PV system can be calculated as,

$$\begin{aligned} \mathit{remaining} = \mathit{initial\ cost} + O\&M - \mathit{utility\ rebate} - \mathit{ITC} - \mathit{state\ tax\ credit} \\ - \mathit{electricity\ savings} \end{aligned} \tag{7}$$

$$\mathit{electricity\ savings} = \sum_{i=1}^{n} E_i \times r \qquad i = 0, 1, 2, 3, 4 \cdots n \tag{8}$$

When *remaining* equals zero, we consider the investment has been paid back, or in other words, it reaches a breakeven point. And the reduced cost for a 4 kW grid-tied PV system before applying the net metering is summarized as Table 5,

Table 5: Detailed PV cost reduction by incentives

Initial Cost	$13,506
Utility Rebate	$2,400
Federal Investment Tax Credit	$3,332
State Tax Credit	$1,000
Subtotal Incentive	$6,731
Remaining Cost	$6,774

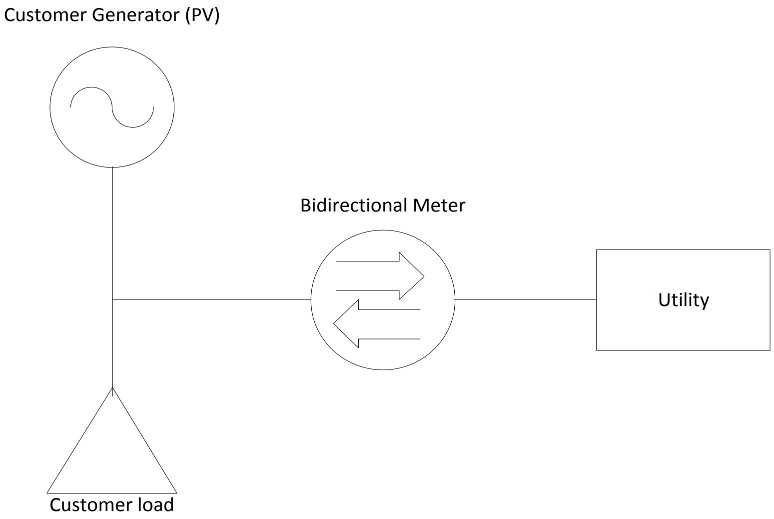

Figure 5 Grid-tied PV system.

2.3 PV Performance with Different Orientations

The orientations and tilt angle of a PV panel are two very important factors in PV system performance. Generally, a surface with tilt angle equal to the latitude of a location receives maximum insolation. Also, a lot of previous research work has been done [16,17,18]. Lewis [16] has given an empirical formula for determining the optimum tilt angle (referred to as β_2 in Figure 6) which suggested that $\beta_2 = \sigma \pm 8°$ based on the examination of 4 locations in USA, where σ is the latitude of the location of the PV system. Various studies have been carried out to investigate the effect of orientation as well [17,19,20,21,22]. Hussein et al. [17] reported that the optimum tilt angle and orientation of PV modules are from $20°$ to $30°$ and south facing. The yearly maximum output energy of PV modules shifted towards the west direction is higher than those shifted towards east.

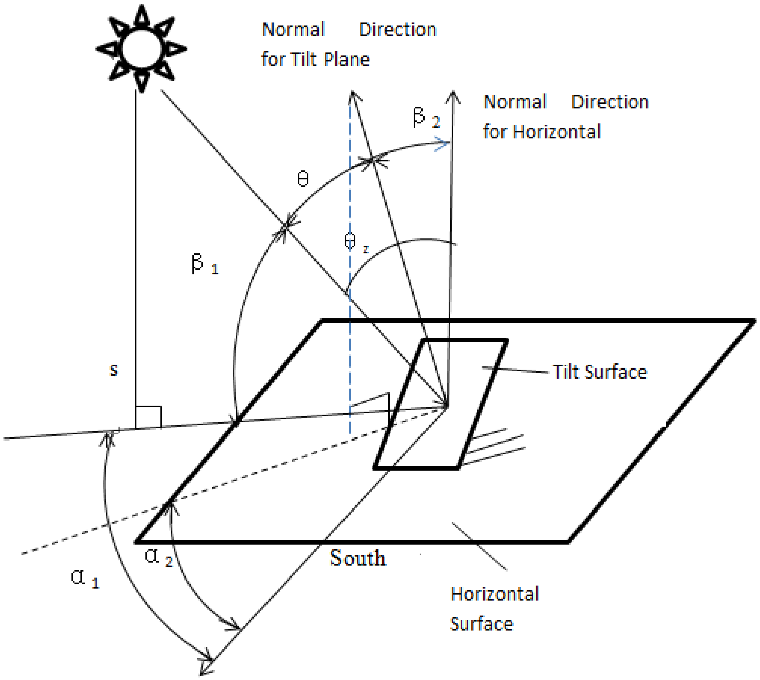

Figure 6 Geometrical relationships between relevant angles.

This chapter investigates the impact of PV orientation and inclination on annual and seasonal bases for the following variables: incident insolation, PV output, PV efficiency, system efficiency, inverter efficiency and PV savings. The seasons are defined as winter (November, December and January), spring (February, March and April), summer (May, June and July) and Autumn (August, September and October).

The study was conducted based on the assumption of a grid-connected residential PV system located in Phoenix (latitude: 34°26'N and longitude: 112° 7'W) within the service area of Arizona Public Service (APS).

2.3.1 Effect of Surface Orientation on Incident Insolation

Generally, the roof angles of residential houses in Arizona are built around 18.4°. But the house can be built facing south, southeast, east, west or southwest. Thus here we assume the tilt angle is 18.4° , and calculate the insolation respected to different orientations.

Data for hourly total solar radiation incident on a horizontal surface is available for many locations in the NREL MIDC. However the in-plane irradiance data need to be calculated.

$$R = R_b + R_d + R_r \tag{9}$$

Where R_b is the beam (direct) contribution, R_d is the sky diffuse component and R_r is the ground reflected radiation, respectively. Figure 7 shows the relationships of the three components of the sun radiation. Therein, the beam radiation which is the main component is varied corresponding to different tilt surfaces.

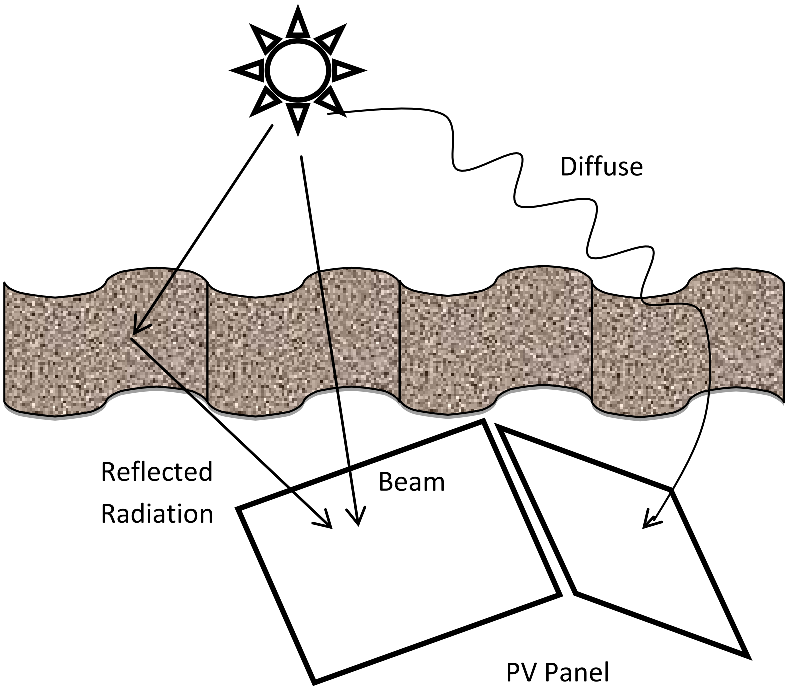

Figure 7 Relationships between the three components of the solar radiation.

And the direct normal insolation received by the inclined tilt surface can be expressed as [23],

$$R_b = R_{DN} \cos(\theta) \tag{10}$$

where R_{DN} is the direct normal radiation, which can be obtained from MIDC. And θ is the collector angle between the sun and normal to the tilt surface, which is expressed as,

$$\cos(\theta) = \sin(\beta_1)\cos(\beta_2) + \cos(\beta_1)\sin(\beta_2)\cos(\alpha_1 - \alpha_2) \tag{11}$$

where α_2 is the tilt rotational angle which is the azimuth angle between normal to the tilt surface and the south direction, and α_1 is the solar azimuth, the angle away from south in the Northern Hemisphere (α_1 is considered to be positive toward the west and negative toward east). And α_1 is given by

$$\cos(\alpha_1) = \frac{\sin(\beta_1)\sin(L) - \sin(\delta)}{\cos(\beta_1)\cos(L)} \tag{12}$$

And the azimuth angle of four seasons is shown in Figure 8. In Equation (12), β_1 is the solar altitude and L is the latitude of the location, and δ is the declination angle.

Therein, β_1 is calculated as,

$$\cos(\beta_1) = \sin(L)\cos(\delta)\cos(H) + \sin(L)\cos(\delta) \tag{13}$$

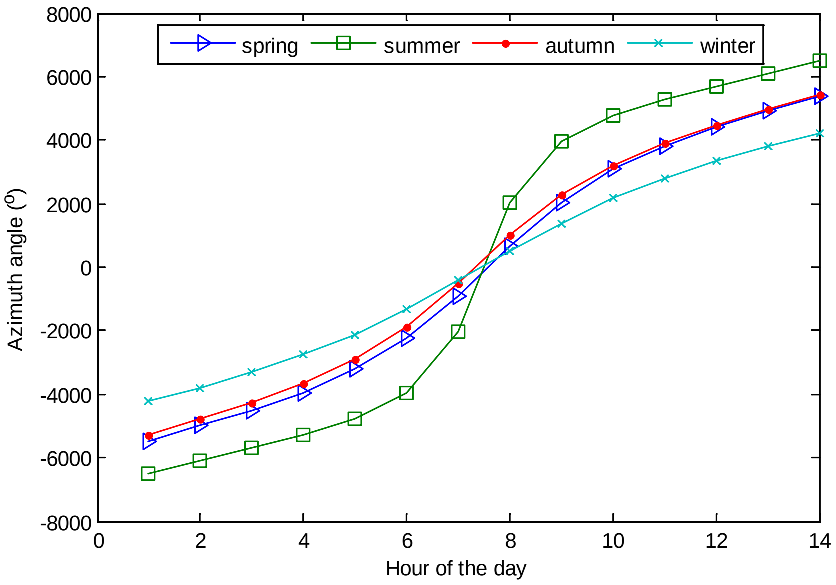

Figure 8 Solar azimuth angle.

And the solar altitude angle of the four seasons in Phoenix is shown as Figure 9. The negative value represents the sun is below the horizon, and once the sun rises up the altitude angle becomes positive. Accordingly, we can see from the graph that summer days have the longest daytime from 6 a.m. to 7 p.m. and winter has the shortest. Hence, in this thesis, we assume solar energy is available during 6 a.m. to 7 p.m.

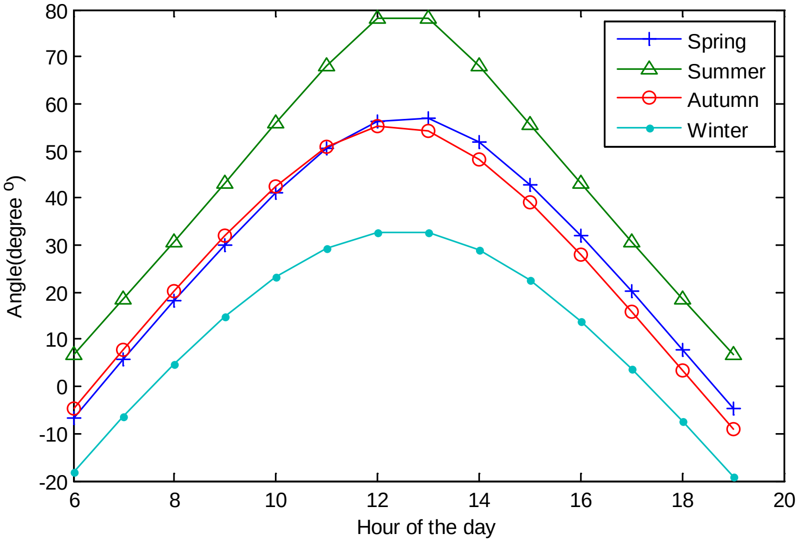

Figure 9 Solar altitude angle.

Other parameters are given by following equations,

The solar angle H: $$H = \frac{(AST - 720)\,\text{min}}{4\,\text{min/ degree}} \qquad (14)$$

where AST is the apparent solar time. The declination angle:

$$\delta = 23.45^\circ \sin\left[\frac{N+284}{365}\times 360^\circ\right] \tag{15}$$

where N is the day number of the year. And in this thesis, March 21, June 21, September 21, and December 21 are chosen to represent the Spring, Summer, Autumn and Winter, respectively. Accordingly, N is 80, 172, 264 and 355.

Apart from the direct radiation, the reflected component and diffuse radiation are given by,

$$R_d = CR_{DN}\left[\frac{1+\cos(\beta_2)}{2}\right] \tag{16}$$

$$R_r = R_{DN}\rho(C+\sin(\beta_1))\left[\frac{1-\cos(\beta_2)}{2}\right] \tag{17}$$

Where C is the ratio of diffuse radiation on a horizontal surface to the direct normal radiation and B is the atmospheric extinction coefficient, Table 6 shows the values of B and C, corresponding to the seasons.

Table 6: Coefficient values in the different season

Season (Date)	B	C
Spring (March 21)	0.156	0.071
Summer (June 21)	0.205	0.134
Autumn (September 21)	0.177	0.092
Winter (December 21)	0.142	0.057

Hence, the diffuse irradiance can be calculated. Figure 10 is the data obtained from NREL. We can see that the diffuse irradiance keeps a very high level (>100 W/m^2) throughout the year.

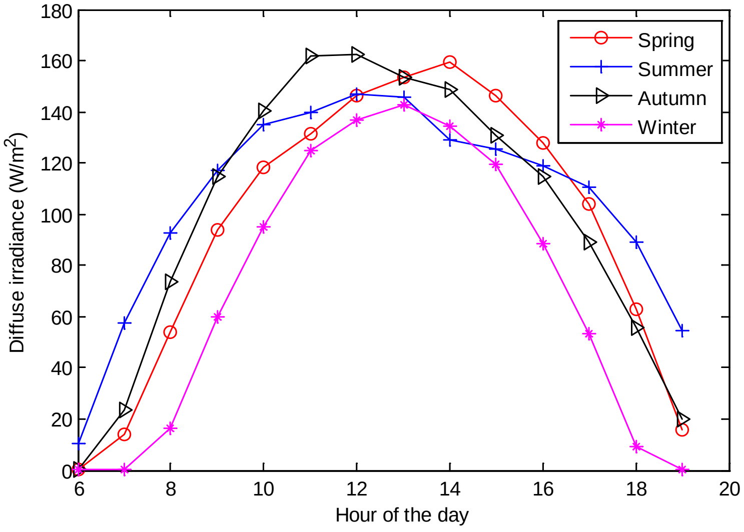

Figure 10 Diffuse irradiance in different seasons.

Finally the total in-plane irradiance can be calculated. As we mentioned, the PV panel can be implemented facing either east, southeast, south, southwest, or west. Consequently, the irradiance is calculated with α_2 equaling -90°, -45°, 0°, 45° and 90°. And the result of the four seasons is shown as Figures 11-14.

From the figures, it can be indicated that in Phoenix, the insolation reaches the strongest level in summer, and reaches the lowest in winter. Moreover, PV panels facing south receive more effective insolation than that of other orientations. This is in compliance with the earth's motion pattern. For the northern hemisphere, the sun is mostly in the north and barely to the south. The graphs are schemed with respect to the local standard time. With apparent solar time, the graphs would display a symmetric pattern towards west and east. The specific data of the irradiance with different orientations for a spring day are listed in Table 7.

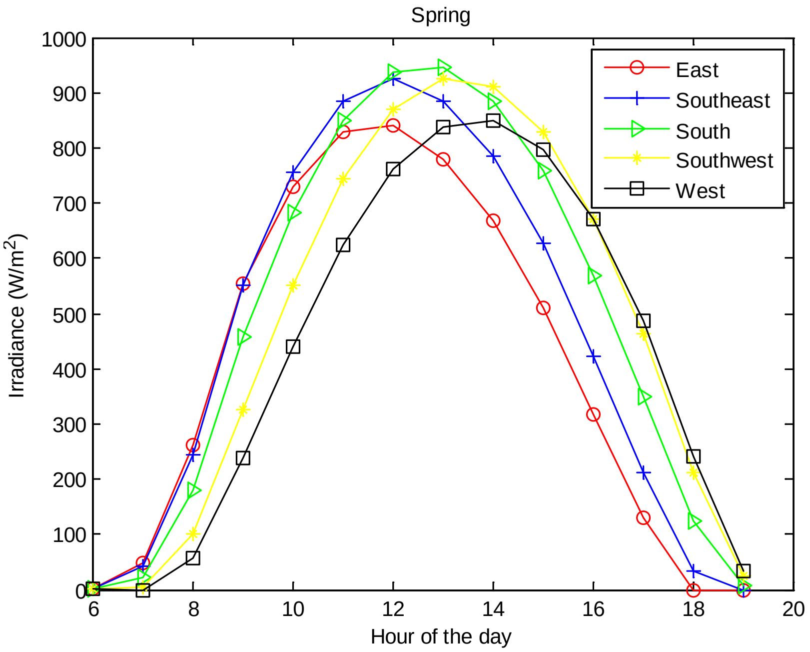

Figure 11 Phoenix irradiance with different orientations in a spring day.

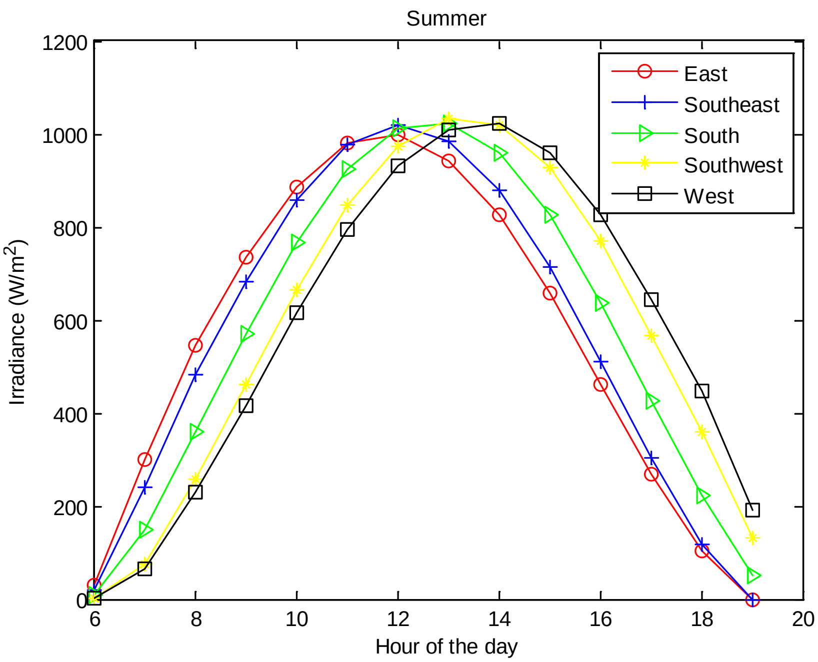

Figure 12 Phoenix irradiance with different orientations in a summer day.

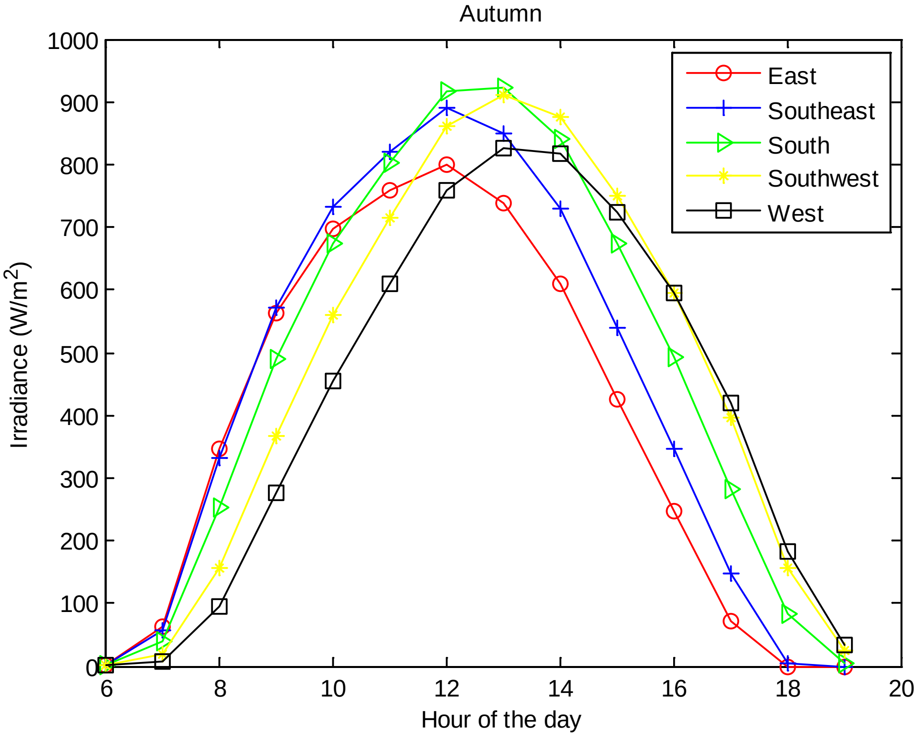

Figure 13 Phoenix irradiance with different orientations in an autumn day.

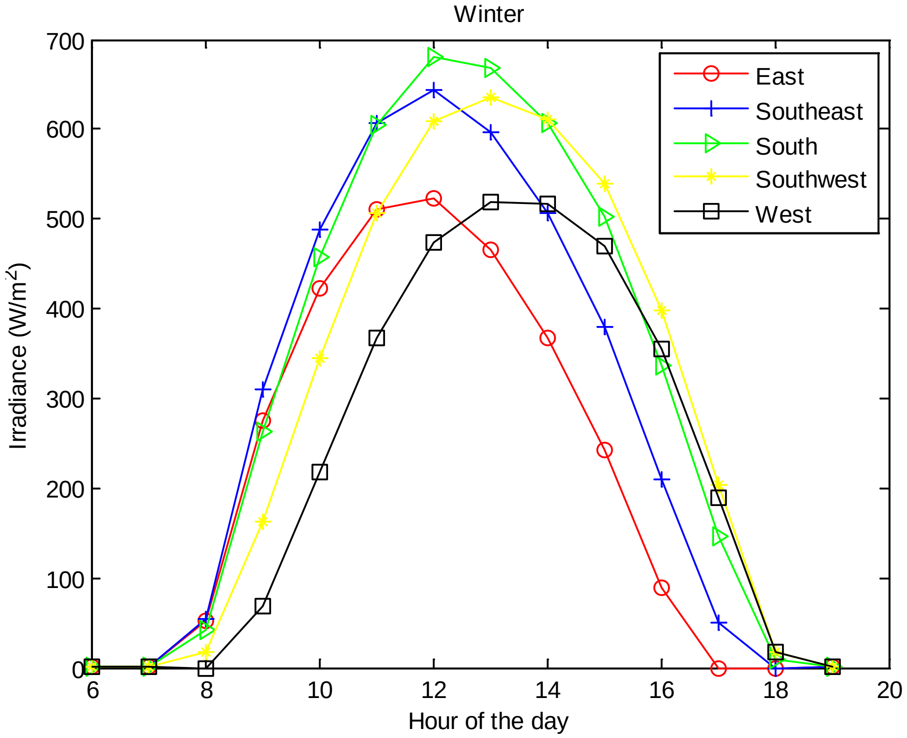

Figure 14 Phoenix irradiance with different orientations in a winter day.

Table 7: The average in-plane insolation with different orientations in spring

Hour of the day	East (W/m^2)	Southeast (W/m^2)	South (W/m^2)	Southwest (W/m^2)	West (W/m^2)
6	0.0	0.0	0.0	0.0	0.0
7	0.2	0.2	0.1	0.0	0.0
8	1.0	1.0	0.7	0.4	0.2
9	2.2	2.2	1.8	1.3	0.9
10	2.9	3.0	2.7	2.2	1.8
11	3.3	3.5	3.4	3.0	2.5
12	3.3	3.7	3.7	3.5	3.0
13	3.1	3.5	3.8	3.7	3.3
14	2.7	3.1	3.5	3.6	3.4
15	2.0	2.5	3.0	3.3	3.2
16	1.3	1.7	2.3	2.7	2.7
17	0.5	0.8	1.4	1.8	1.9
18	0.0	0.1	0.5	0.8	1.0
19	0.0	0.0	0.0	0.1	0.1
20	0.0	0.0	0.0	0.0	0.0

2.3.2 PV Output

With the PV model presented previously, the generation output is obtained with simulation. Table 8 and Figure 15 show the generation produced by the PV panel with orientations varying from east to west in Phoenix. It is obvious that a PV panel tilted towards south gains the most generation due to the higher in-plane insolation level. And also, a PV panel towards west produces more generation than that of east. That is the consequence of higher solar radiation level in the afternoon according to the local standard time. And Phoenix is in the west side of the Mountain time zone.

Table 8: PV generation (kWh) seasonally and annually with different orientations

orientation Season	East	Southeast	South	Southwest	West
Spring	22.6	25.3	26.9	26.4	24.0
Summer	30.8	31.0	31.6	32.2	32.5
Autumn	21.2	24.0	25.8	25.4	23.1
Winter	11.7	15.3	17.2	16.1	12.7
			x 91 days		
Annual	7930	8798	9337	9214	8491

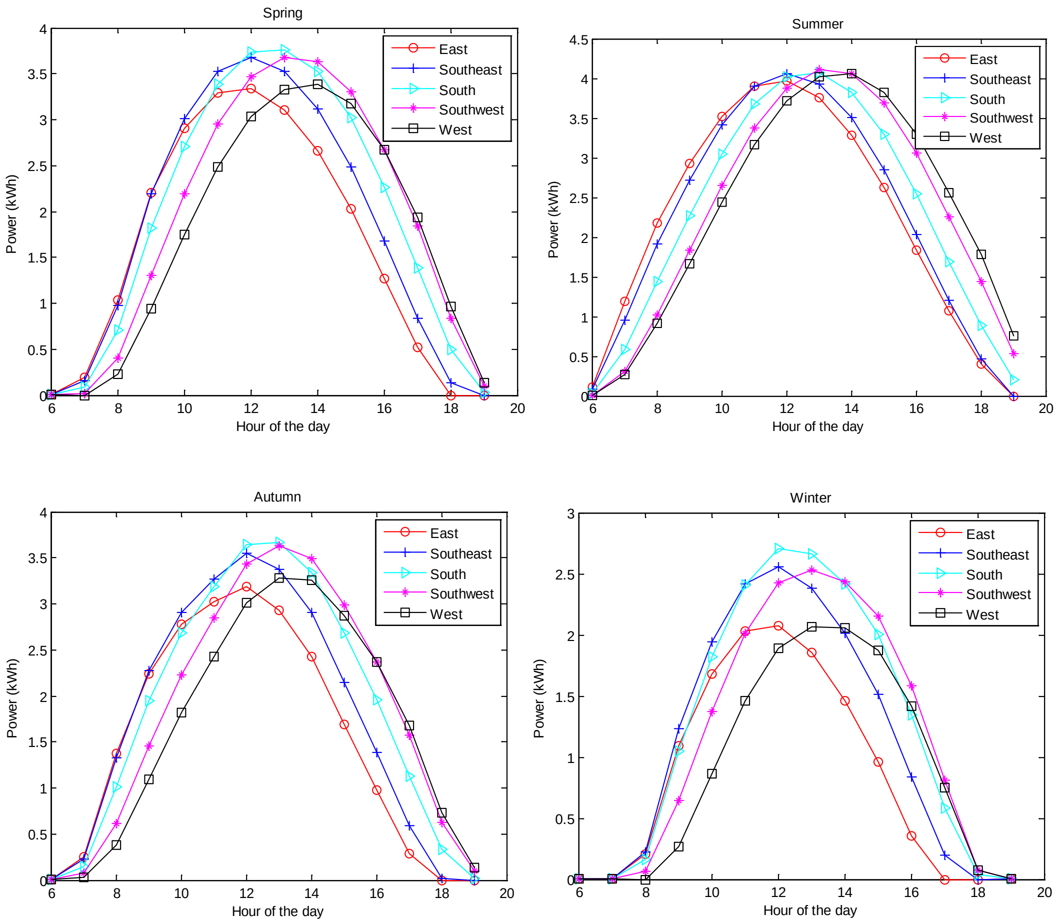

Figure 15 Hourly PV generation seasonally with different orientations for a 4 kW system.

2.3.3 PV Savings

For homeowners, the electricity tariff has two alternative rate plans as listed in Table 9. One depends on the time of use (TOU), based on off-peak and on-peak time periods. With TOU plan, PV displaces more economically value when the PV system reduces the peak load demand due to the more expensive utility electricity. For the other, named flat rate plan, residential users pay a constant electricity rate throughout the billing cycle. With the flat rate plan, best orientation corresponds to the maximum total annual PV generation.

Table 9: Utility rate plans

Type of Tariff	**Time period**		**Rate (¢/kWh)**
Flat rate		Flat rate plan	9.397
TOU	Winter	7 p.m. to 12 p.m. (Mon.-Fri., November-April) and weekends	6.124
		12 p.m. to 7 p.m. (Mon.-Fri., November-April)	19.825
	Summer	7 p.m. to 12 p.m. (Mon.-Fri., May-October) and weekends	6.126
		12 p.m. to 7 p.m. (Mon.-Fri., May-October)	24.445

a. Flat rate plan

Table 10 and Figure 14 show the annual savings with different orientations. It is clear that for the flat rate plan the annual savings reaches the maximum value towards south due to the largest power generation as referred to in Table 10 and Figure 16. Also, from the seasonal result and figures, we can see that PV electricity savings is similar for the same orientation towards east and west from south (namely west and east, southwest and southeast). However, the savings towards west are still around 5% larger than that towards east due to the higher PV output towards west as mentioned in Section 2.3.2.

Table 10: PV electricity savings ($) per day seasonally and annually with different orientations for flat rate plan

orientation	East	Southeast	South	Southwest	West
Spring	2.5	2.8	3.0	2.9	2.6
Summer	3.4	3.4	3.5	3.5	3.6
Autumn	2.3	2.6	2.8	2.8	2.5
Winter	1.3	1.7	1.9	1.8	1.4
			x 91 days		
Annual	872	968	1027	1014	934

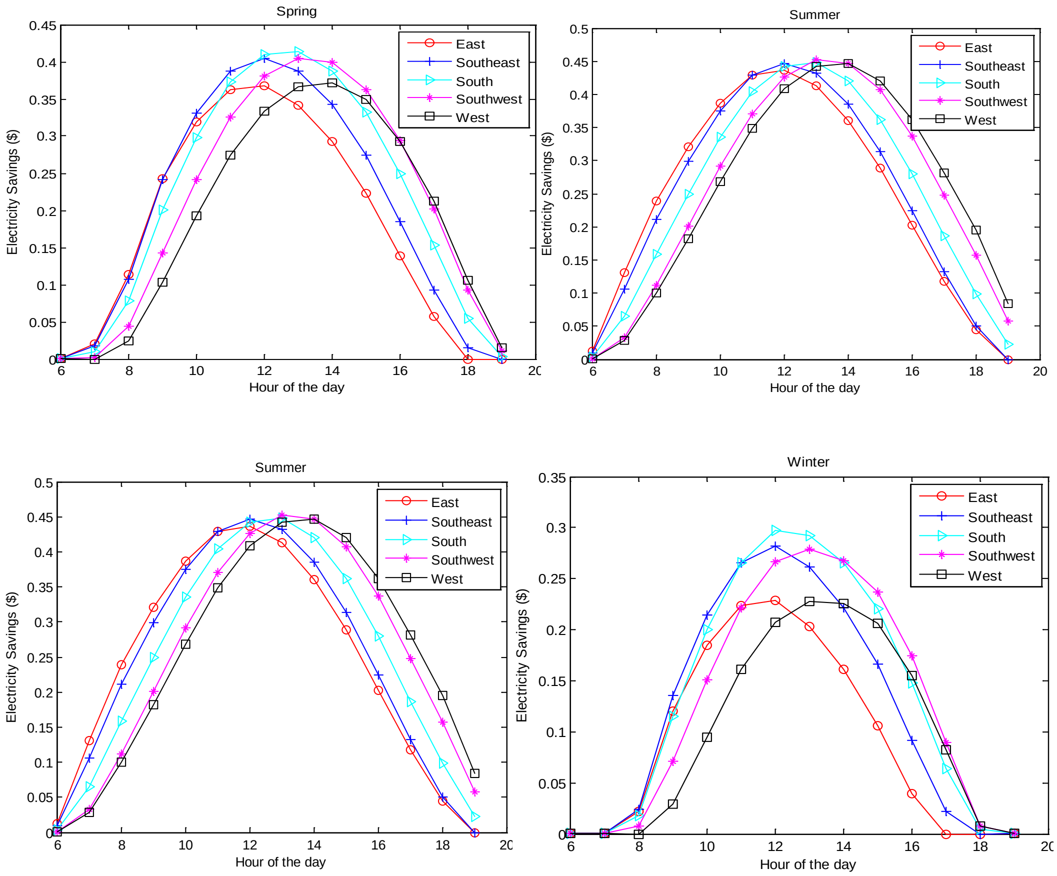

Figure 16 Hourly electricity savings with flat rate plan seasonally with different orientations.

b. TOU plan

For the TOU plan provided in Table 11, it can be indicated from Table 11 and Figure 15 that the maximum annual PV savings is $1476 for a surface with azimuth angles of 45°, namely southwest and followed by west, south, southeast and east. The results show that the annual PV electricity savings is always higher for tilted surfaces facing the same angle towards west than east. Specifically, the PV saving towards southeast is 23% lower than southwest, and PV savings towards east is 38% lower than west. This is a consequence of the time-dependent rate plan, which makes the generation in the afternoon, namely the peak time, more valuable. And from Figure 17, it can be seen that the PV generation output curve towards west is more oblique in the afternoon than that towards west. That means PV towards west generates much more valuable electricity than that towards east.

Table 11: PV electricity savings ($) per day seasonally and annually with different orientations for TOU plan

orientation	East	Southeast	South	Southwest	West
Spring	2.0	2.5	2.9	3.1	2.9
Summer	3.4	3.6	4.1	4.5	4.6
Autumn	1.9	2.4	2.9	3.0	2.8
Winter	0.9	1.5	1.9	1.9	1.5
			x 91 days		
Annual	1031	1196	1381	1476	1421

Now compare Table 10 to Table 11, it is obvious that the maximum PV savings with the flat rate plan is 43.7% lower than that with TOU plan. And the PV savings with TOU is also higher than any identical orientation for the flat rate plan.

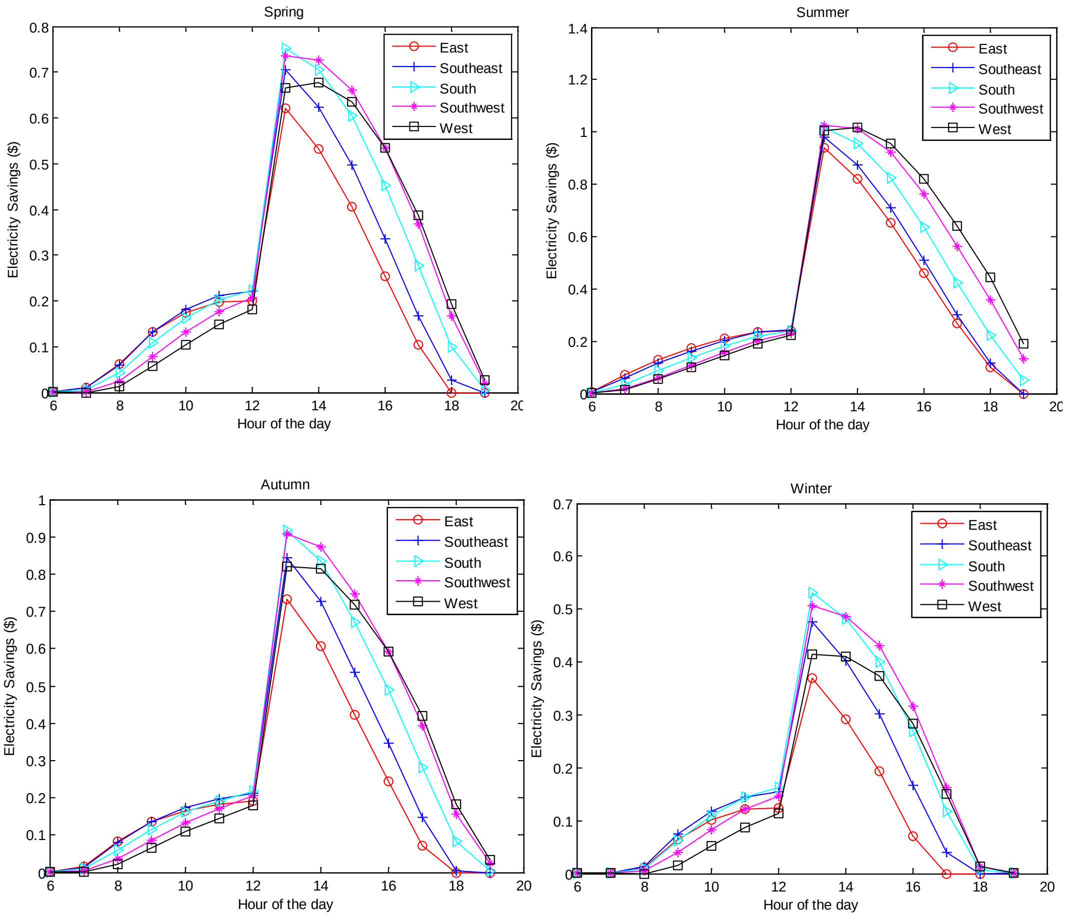

Figure 17 Hourly electricity savings with TOU seasonally with different orientations.

2.3.4 Payback Condition

As we have assumed, a 4 kW PV system in Phoenix with service from APS is selected to calculate the payback condition. Also, as referred to in Table 3, the system cost is around $3.4/W and the state tax credit is 25%. The breakeven point of both the flat rate plan and TOU plan are listed in Table 12 and the return of investment is shown in Figures 18-19.

For the flat rate plan, we can see that the breakeven period displays a symmetric pattern. And the fastest way to pay back the investment is to implement the PV panel towards southeast, south or southwest. Even though, with Figure 16, we know PV towards south still leads to a higher investment return every year, then followed by southwest, southeast, west and east.

As for the TOU plan, the fastest to reach the breakeven point is the PV towards south, southwest and west, this corresponds to the PV electricity savings pattern in Table 8.

Meanwhile, comparing Figure 18 and Figure 19, the TOU plan leads to more significant differences between the different orientations. The slope with PV towards west is steeper than that towards east, which means a much faster speed of investment return. Specifically, for either rate plan, the initial cost is \$3.4/W*4kW=\$13,600.

Table 12: Breakeven period (years) for a 4 kW PV system

Orientation Tariff Type	East	Southeast	South	Southwest	West
Flat rate	10	9	9	9	10
TOU	9	7	6	6	6

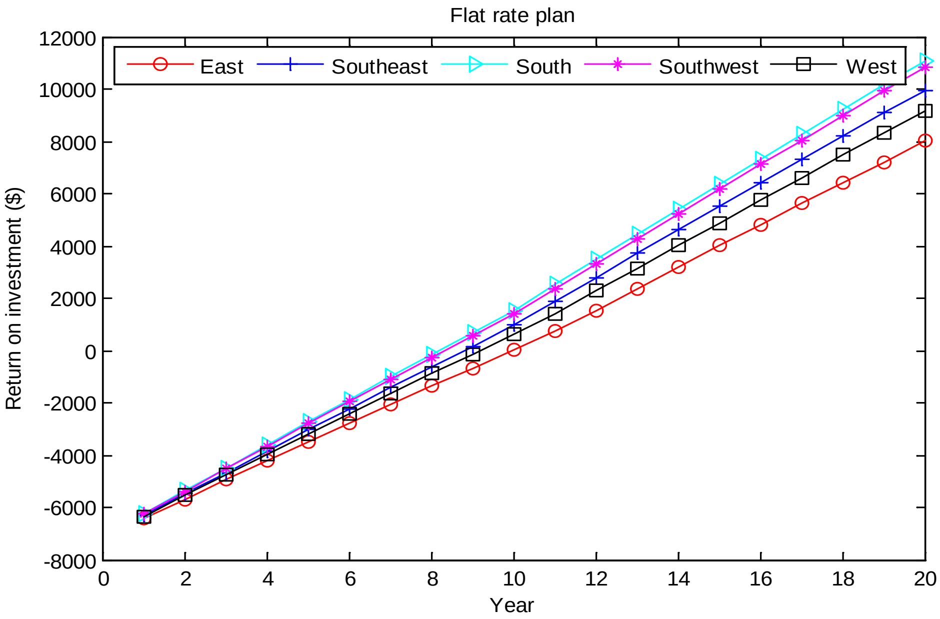

Figure 18 Return on investment for flat rate plan.

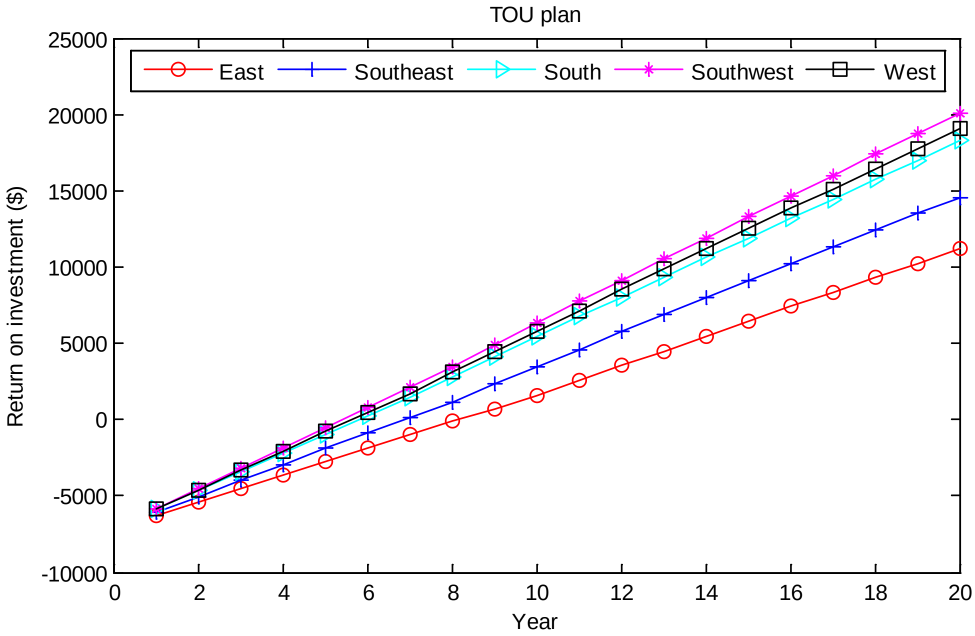

Figure 19 Return on investment for TOU plan.

3. WIND POWER

Wind power grid-connected systems are widely installed internationally. Figure 20 shows a typical grid-connected wind power system.

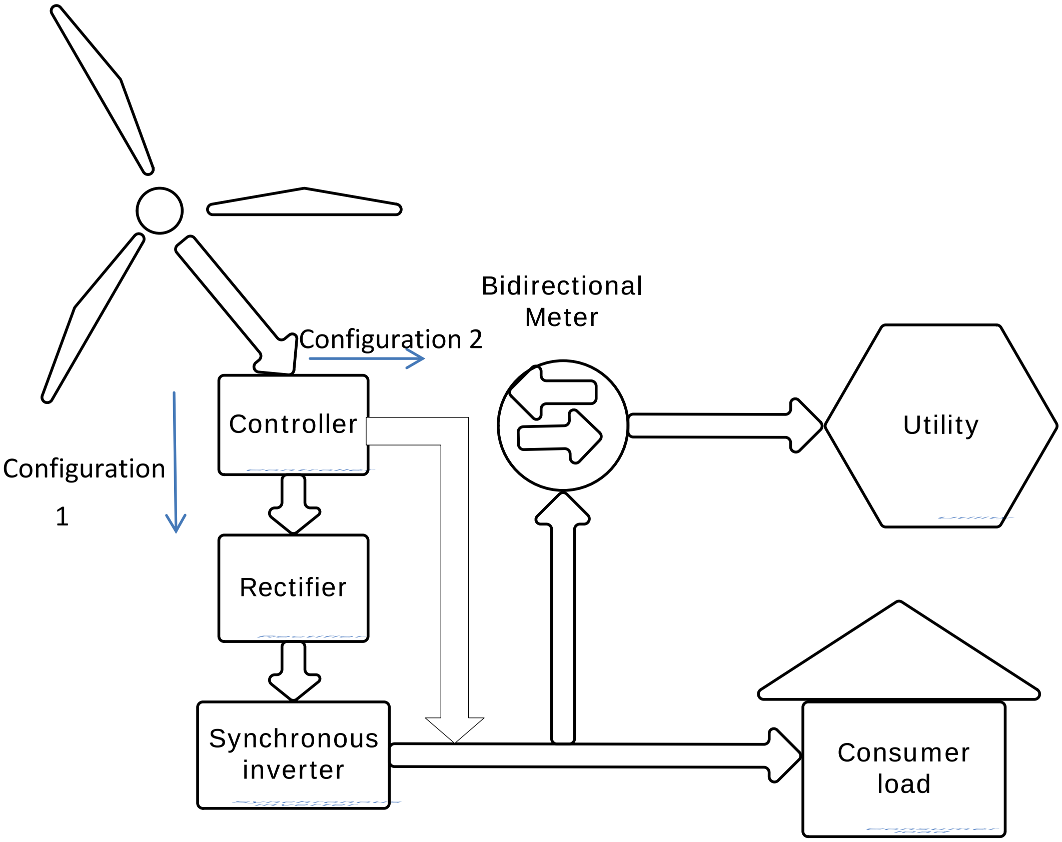

Figure 20 Small wind turbine configurations.

There are two common configurations for grid-connected wind turbines shown in Figure 20, which is distinguished by the type of output of the wind generator. For configuration 1, the wind turbine generator is either a permanent-magnet alternator or wound-field synchronous generator. And the output is variable voltage, variable frequency alternating current (AC) (usually three phase), which needs to be conditioned through an inverter, and then fed to the utility grid through a bidirectional meter. For configuration 2, the inductive generator provides reliable quality, grid frequency output AC power. That means the inverter is unnecessary.

3.1 Wind Turbine Sizing

Wind-generator sizing requirements depend on the average wind speed of the location and the renewable energy consumption demand expected to be met with the wind generator.

For the U.S., an average home electricity consumption is around 1,000 kWh/month and the farm could use 100,000 kWh/month [24]. Thus, general figures indicate that a wind turbine rated at power output between 1 kW to 5 kW but even up to 15 kW would be suitable. And those sizes of wind turbines are called small wind turbine (≤100 kW).

3.2 Small Wind Turbine

During 2010, more than 25 MW of small wind turbines were installed in the U.S., which is a 26% growth from 2009. And compared to 5 years ago, the increase of annual installation capacity is almost eight-fold [25]. The total installed small turbine capacity has increased to 179 MW (144,000 turbines).

And according to the data [25] reported from 22 manufacturers in the U.S., a significant trend of shifting from off-grid units to grid-connected units has emerged in recent years as the boom of grid-tied energy in recent years. Ninety percent of the wind turbine models sold in the U.S. was grid-tied.

3.2.1 SWCC (Small Wind Certification Council)

The Small Wind Certification Council (SWCC), an independent certification body, certifies small wind turbines that meet the requirements of the American Wind Energy Association (AWEA) Small Wind Turbine Performance and Safety Standard [26].

According to the standard, the SWCC certify the parameters including rated annual energy output, the total energy that produced during one year with an average wind speed of 5 m/s (11.2 mph); AWEA Rated Sound Level, the sound pressure level (dBA) not exceeded by the wind turbine 95% of time at a distance of 60 meters from rotor with a hub height annual average wind speed of 5 m/s (11.2 mph); and AWEA Rated Power, the wind turbine power output at 11 m/s (24.6 mph).

With the SWCC certificate we can easily understand the wind turbine performance. According to the certified turbines obtained from the SWCC, the

Skystream 3.7 from Southwest Windpower is chosen in this work for a home user, and Excel 10 from Bergey Windpower Co. is selected for a farm.

3.2.2 Skystream 3.7

The Skystream 3.7 is the first fully-integrated and grid-tied wind turbine that designed for residential use. And it has the controls and inverter built in. Thus it is expected to provide quiet, clean electricity in very low winds. And unlike many other turbines, the Skystream 3.7 is the downwind type without a tail rudder to keep it facing into the wind. The key parameters of the wind turbine are listed in Table 13.

Table 13: Specifications of Skystream 3.7 [27]

AWEA Rated Annual Energy at 5 m/s	3420 kWh
AWEA Rated Sound Level	41.2 dB(A)
AWEA Rated Power at 11 m/s	2.1 kW
Cut-in Wind Speed (power production starts)	8 mph (3.5 m/s)
Cut-out Wind Speed	27 mph (60 m/s)
Rated Wind Speed	29 mph (13 m/s)

3.2.3 Bergey Excel 10

The Bergey Excel is designed for high reliability, low maintenance, and automatic operation in adverse weather conditions. It can be operated based on both battery charging and on-grid. The Excel 10 is most often installed on a guyed-lattice tower, which is available in heights of 18 m (60 ft.) to 43 m (140 ft.). The key parameters of the wind turbine are listed in Table 14.

Table 14: Specifications of Bergey Excel 10 [28]

AWEA Rated Annual Energy at 5 m/s	13,800 kWh
AWEA Rated Sound Level	42.9 dB(A)
AWEA Rated Power at 11 m/s	8.9 kW
Cut-in Wind Speed	2.5 m/s (5 mph)
Cut-out Wind Speed	None
Rated Wind Speed	16 m/s

3.3 Wind Modeling

The power output of a WTG (Wind Turbine Generator) can be determined using the functional relationship between the power output of the WTG and the wind speed as shown as Equation (18) [29].

$$P(V_w) = \left\{ \begin{array}{ll} 0 & 0 \le V_w \le V_{ci} \\ (A + B \times V_w + \mathrm{C} \times V_w^{\ 2}) \times P_r & V_{ci} \le V_w \le V_r \\ P_r & V_r \le V_w \le V_{co} \\ 0 & V_w \ge V_{co} \end{array} \right\} \tag{18}$$

Where,

V_w: wind speed (m/s)

P_r: rated power output;

V_{ci}: cut-in wind speed;

V_r: rated wind speed;

V_{co}: cut-out wind speed.

The constants *A*, *B*, and *C* may be found as functions of V_{ci} and V_r with the following equations [30]:

$$
\begin{aligned}
A &= \frac{1}{(V_{ci}-V_r)^2}\left[V_{ci}(V_{ci}+V_r)-4V_{ci}\frac{(V_{ci}-V_{\mathrm{r}})^3}{2V_r}\right]\\
B &= \frac{1}{(V_{ci}-V_r)^2}\left[4(V_{ci}+V_r)\frac{(V_{ci}+V_{\mathrm{r}})^3}{2V_r}-(3V_{ci}+V_{\mathrm{r}})\right]\\
C &= \frac{1}{(V_{ci}-V_r)^2}\left[2-\frac{(4V_{ci}+V_{\mathrm{r}})^3}{2V_r}\right]
\end{aligned}
\tag{19}
$$

Thus using the manufacturer data for the Skystream 3.7, the constants are determined here as,

A = 5.675, *B* = 142.5, *C* = -12.59

Likewise, the coefficients for Bergey Excel 10 are,

A = 4.331, *B* = 83.330, *C* = -5.799

3.4 Wind Power System Cost in Arizona

3.4.1 System Initial Cost

From the manufacturer, the Skystream 3.7 wind turbine is $15,210, an all-inclusive wind generator (with controls and inverter built in). Also according to the manufacturer instruction, the other critical component, a 70 ft. guyed tower, is included. And the technicians have been approximated to be $1500. As a result the initial cost is around $16,710. Note that these costs have been used for these analyses but will change in the future.

3.4.2 Incentives

The incentives which will be discussed include utility cash rebate, net metering, sales tax incentives, and property tax incentives. And the specifics can be found under the DSIRE website. In this case, we assume the homeowner uses APS (Arizona Public Service) as the utility company. And the applicable incentives are listed in Table 15.

Table 15: Incentives available with APS

Federal Incentive tax credit	30%
Arizona State tax credit	25% with a cap of $1,000
Utility rebate (APS)	$2.25/ kW with a maximum of 50% of the initial cost

1) Cash Incentives

APS provides a rebate of $2.25/W for grid-tied wind systems (residential and non-residential) based on rebate plan ERP-6. That means, under optimal conditions, a homeowner installing a Skystream 3.7 wind turbine, which is rated at 2.4 kW, can receive a rebate equaling $ 5,400.

2) Federal Investment Tax Credit

The $5,400 utility rebate needs to be subtracted from the initial cost of the system to determine the cost basis. As a result the cost basis is $11,310 and the ITC is $3,393.

3) State Tax Credit

The Arizona residential Solar and Wind Energy Systems Tax Credit [31] allows against the taxpayer's personal income tax in the amount of 25% of the cost of a solar or wind energy device, with a $1,000 maximum allowable limit, regardless of the number of energy devices installed. As a result, a homeowner with a Skystream 3.7 wind turbine can receive a tax credit of $1,000.

Thus, the cost of a grid-tied power system based on Skystream 3.7 can be reduced to $6,917, as summarized in Table 16,

Table 16: Detailed wind system cost reduction by incentives

Initial Cost	$1,6710
Utility Rebate	$5,400
Federal Investment Tax Credit	$3,393
State Tax Credit	$1,000
Subtotal Incentive	$9,800
Remaining Cost	$6,910

3.4.3 Electricity Savings

As we mentioned previously, with net metering, homeowners are allowed to send back the excess power to the utility and obtain corresponding electricity savings based on different rate plans.

1) Flat Plan

For the flat rate plan, the ERP-6 net metering is chosen. It allows the homeowner to sell the excess power back to APS at a rate of retail price, which is approximately \$0.1/kWh.

Based on the Wind Energy Resource Atlas of the United States, Arizona has locations of up to Class 5 wind resources. Therefore, payback was calculated as a function of annual average wind speeds of 5.4 m/s, 5.8 m/s and 6.2 m/s.

With Equation (18) the annual output of the wind system can calculated and the result is shown in Table 17. For example, under the condition of a wind speed of 5.4 m/s, a homeowner in Arizona (e.g. Flagstaff) with Skystream 3.7 can generate about 8,733 kWh of power annually. And that means a \$873 savings annually, as shown in Figure 21.

Table 17: Power generation and electricity saving with different wind speeds

Wind Speed (m/s)	Power Generation Annually (kWh)	Electricity Saving ($)
5.4	8733	873.3
5.8	9180	918
6.2	10027	1002.7

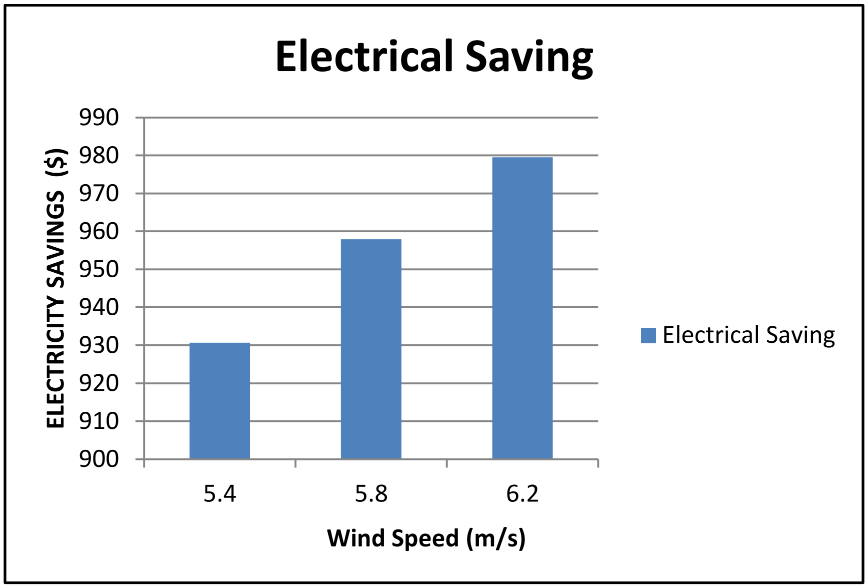

Figure 21 Annual electrical savings with different wind speeds.

3.4.4 Calculation of the Breakeven Point

Assume the annual operation and maintenance costs were 1% of the installed turbine system costs. And there is also a derate of the wind turbine outputs of 0.5% every year.

Given the combination of the up-front rebate, the ITC, and the value of the retail electricity savings, it turns out that it takes 11 years for a wind power system based on Skystream 3.7 to reach a breakeven point under the average wind speed of 5.4 m/s. And in 30 years it will earn $12,386. The process of reaching a breakeven point is shown as Figure 22.

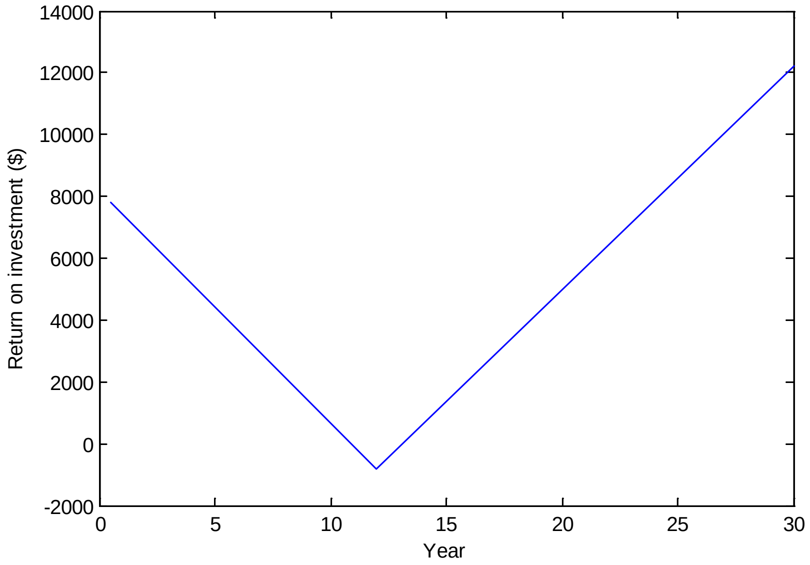

Figure 22 The breakeven point and return on investment with wind speed of 5.4 m/s in Arizona.

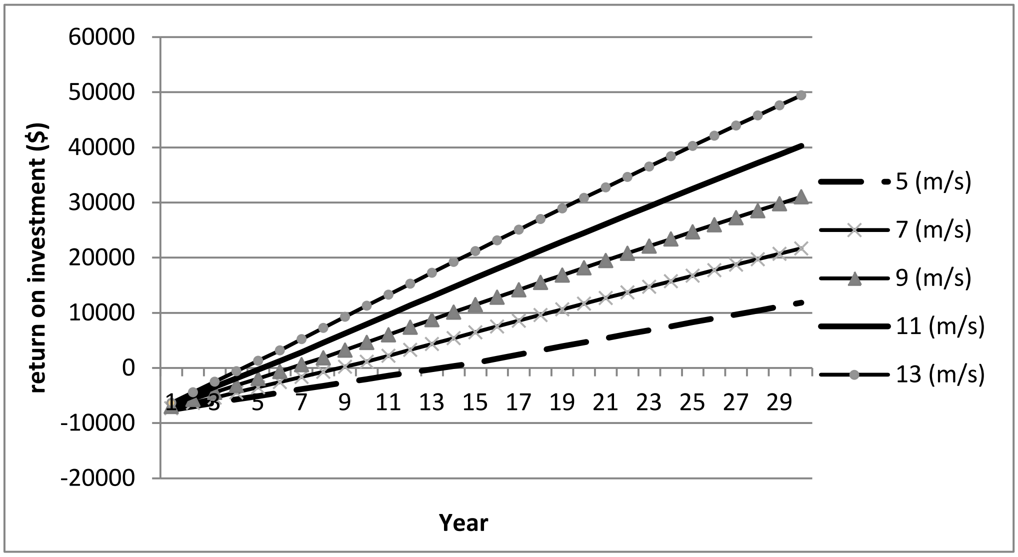

Figure 23 Return on investment with different wind speeds.

We can see from Figure 23 that the pay-back year for wind speeds of 5, 7, 9, 11, and 13 m/s, is respectively, 14, 9, 7, 6, and 5 years. Hence, increasing the wind speed contributes to shorter payback duration. And the main reason that makes this difference is that higher wind speeds lead to higher electrical savings.

3.5 Wind Power System Cost in California

3.5.3 Incentives

Incentive programs in California include an Emerging Renewables Program, sales tax incentives, property tax incentives and net metering. Table 18 shows an incentive program in California with San Diego Gas & Electric.

Table 18: Incentives available with San Diego Gas & Electric

Federal Incentive Tax credit	30%
State Rebate Program	$3.00/W rebate for first 10 kW and $1.50/W for increments with a cap of 30 kW

1) State rebate

Based on the Emerging Renewables Program, California provides a $3.00/W rebate for first 10 kW and $1.50/W for increments. (This rebate is reported to decline to $2.50/W on May 8, 2012.) And according to the list of eligible equipment from the California Energy Commission (CEC) [32], the output power rating at 11 m/s will be applied as the system size for calculating the incentive, which can be obtained from SWCC. And it is 2.1 kW for Skystream 3.7. As a result, the rebate is $6,300.

2) Federal Investment Tax Credit (ITC)

The basis cost is reduced by the $6,300 up-front rebate. This translates to an ITC cost basis of $10,410. As a result, the ITC is $3,123.

3.5.4 Electricity Savings

In California, the Assembly Bill 920 authorizes utilities to compensate Net Energy Metering (NEM) customers for excess generation at the end of their true-up period. And the compensation price is around 3.6 cents per kWh. The true-up period rate is given in Table 19.

Based on the Wind Energy Resource Atlas of the United States, California has locations of up to Class 6 wind resources. Therefore, payback was calculated as a function of annual average wind speeds of 5 m/s, 7 m/s, 9 m/s, 11 m/s and 13 m/s.

Table 19: True-up period rate [33]

Month	Year	Price($/kWh)
March	2012	0.03551
February	2012	0.03602
January	2012	0.03658
December	2011	0.03699
November	2011	0.03711
October	2011	0.03740
September	2011	0.03692
August	2011	0.03661
July	2011	0.03639
June	2011	0.03648
May	2011	0.03653
April	2011	0.03673
March	2011	0.03775
February	2011	0.03876
January	2011	0.03980

a. With wind speed of 6 m/s

With Equation (18) the annual output of the wind system can be calculated and shown in Table 20. Under the condition of a wind speed of 5 m/s, a homeowner in California with a Skystream 3.7 can generate about 9600 kWh power annually. And that means a $384 savings annually. Hence, the payback period can be calculated and plotted as Figure 24.

Table 20: Power generation and electricity saving with different wind speed in California

Wind Speed (m/s)	Power Generation Annually	Electricity Saving ($)
6	9600	355.2
7	11321	451.1
9	16702	618
11	22027	815
13	28189.2	1043.2

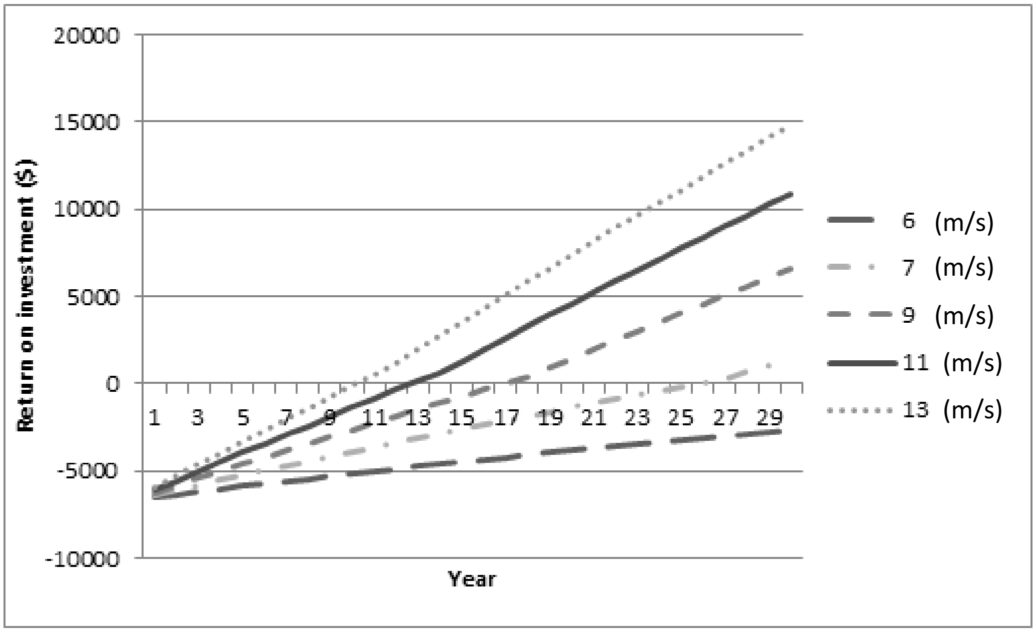

Figure 24 The breakeven point and return on investment in California

4. PV-Wind Hybrid System

In this chapter, a solar-wind hybrid system is investigated. It is a grid-tied residential size system combining PV panels and wind turbines. The main purpose of the research focuses on the effectiveness of each component within the whole hybrid system.

4.1 A Case Study

As we mentioned earlier, California now has one of the most favorable renewable incentives environment of all the states in U.S. Thus, California was chosen to perform the hybrid system payback analysis.

The other very important parameter to assess a hybrid system is the condition of the energy resource, namely, the solar and wind energy.

a) Solar energy

From the PV Solar Radiation Static Maps (10 km) [34] from NREL, it can be seen that California has solar energy with an annual radiation around 6 kWh/m^2 per day. And 90% of the California residents can obtain radiation higher than 5 kWh/m^2 per day. This is ideal for a PV panel.

b) Wind energy

Wind energy is more geographically varied, which means the performance of wind turbines is more regionally dependent.

Wind resources are classified into seven classes, each covering a range of annual average wind speeds (Class 1 representing the lowest wind speed). In general, a Class 2 (4.4 to 5.1 m/s at 10 m) resource or higher is required for effective use of wind due to the requirement of cut-in wind speed of the turbines.

According to NREL, more than 13,000 of California's wind turbines, or 95 percent of all of California's wind generating capacity and output, are located in three primary regions: Altamont Pass (east of San Francisco - a portion of which is shown in Figure 25 [35] from NREL), Tehachapi (southeast of Bakersfield) and San Gorgonio (near Palm Springs). Altamont (Latitude: 37° 41' 35" N; Longitude: 121° 36' 34" W) was chosen as a location to do the economic analysis under good wind conditions. From Figure 25, we can see that the Altamont area has a Class 6 (6.4 m/s to 7.0 m/s) wind resource which is much higher than the surrounding regions.

However, most parts of California are not so windy and have Class 2 or 3 wind resources. To obtain realistic results, Midhill (Latitude: 35° 07' 23" N; Longitude: 115° 24' 41" W) was selected as another analysis location. Figure 25 shows the average annual wind speed in southern California, we can see Midhill has a Class 3 (5.1 to 5.4 m/s at 10 m).

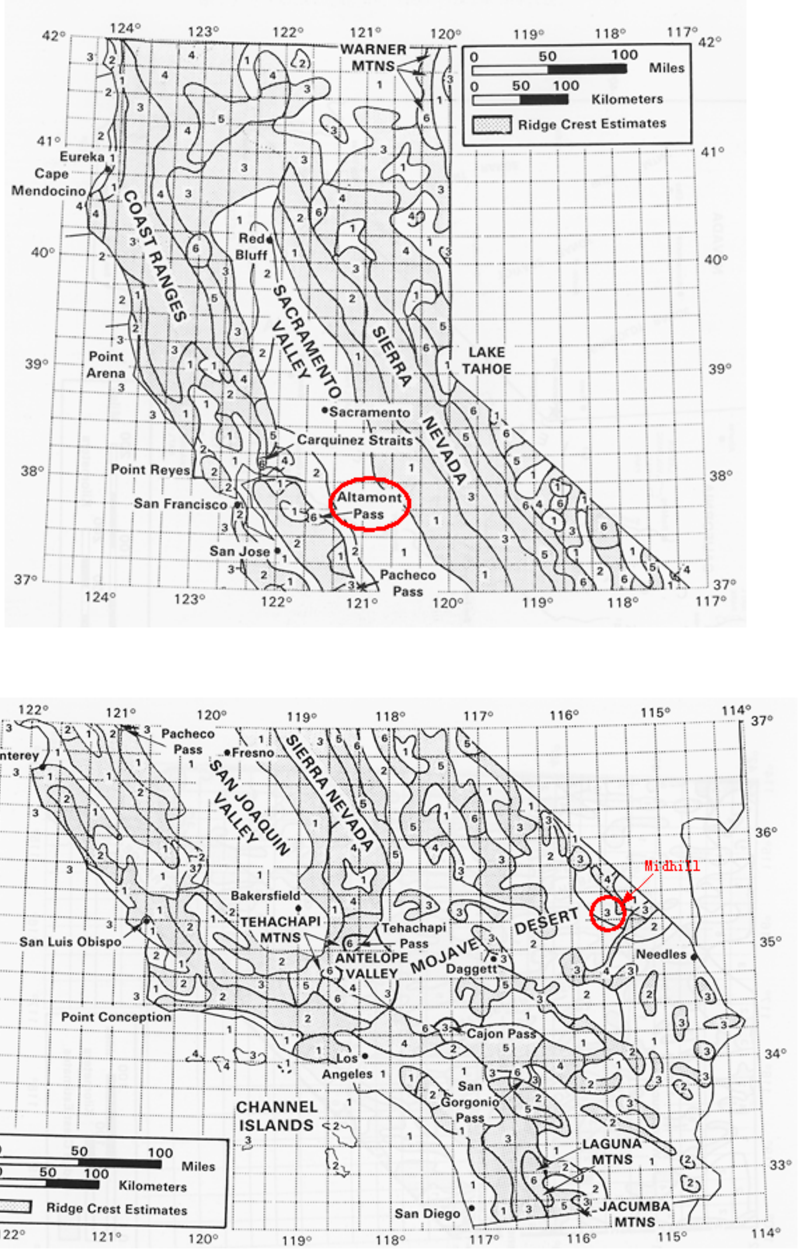

Figure 25 Northern and Southern California annual average wind power.
(*Note: the numbers in the graph represent the class of the wind resources.)

4.1.1 Initial Data Acquisition

The hourly average wind speed and solar radiation data can be obtained from the WRCC (West Region Climate Center) as shown in Figure 26 and Figure 27. And from the graphs, it can be seen that in Altamont both the wind and solar energy reach the highest values in summer and lowest in winter. However in Midhill, the least windy season is Autumn. And summer still exhibits the most sunshine.

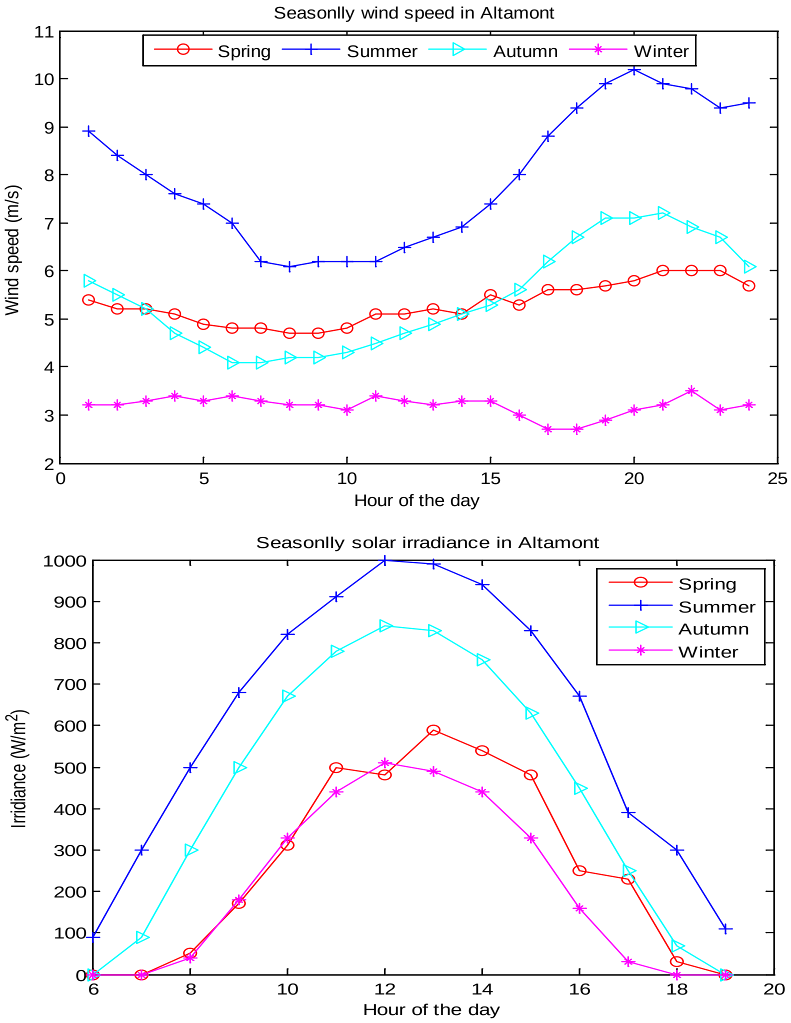
Seasonlly wind speed in Altamont

Seasonlly solar irradiance in Altamont

Figure 26 Seasonal wind speed and solar irradiance in Altamont.

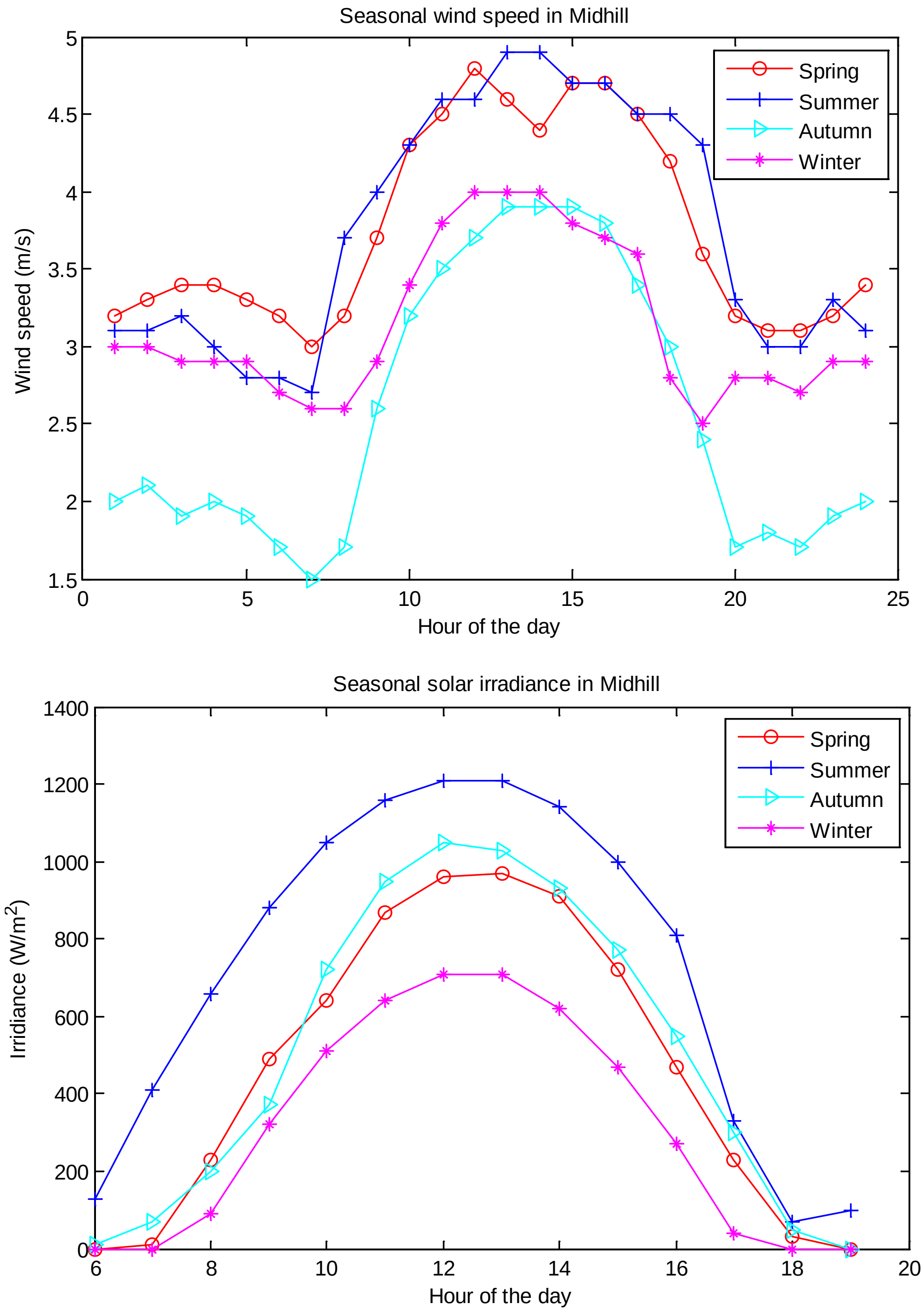

Figure 27 Seasonal wind speed and solar irradiance in Midhill.

Figure 28 shows the distribution of wind speed over a year in Altamont. The average wind speed is 5.5 m/s, with a standard deviation of 1.91 m/s and the median is 5.2 m/s. The maximum wind speed is 10.2 m/s which is observed in the summer evening. As we know, the output of a wind turbine is approximately proportional to the cube of wind speed. Thus with the average hourly data classified by seasons, the energy output potential of a wind turbine is underestimated.

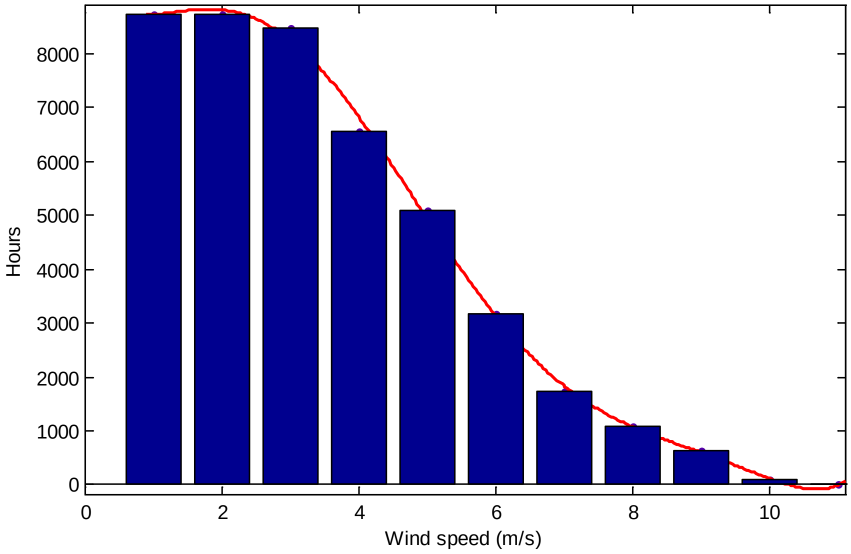

Figure 28 Cumulative probability distribution of wind speed profile in Altamont.

4.1.2 Analysis Process

The system performance is analyzed with the process shown in the flowchart as Figure 29. The wind and solar radiation data of Altamont are applied to the wind turbine and PV generation models as mentioned in Section 3.1 and Section 4.1 to simulate the system generation performance. Then with the corresponding renewable incentives, the payback period and return on investment can be calculated.

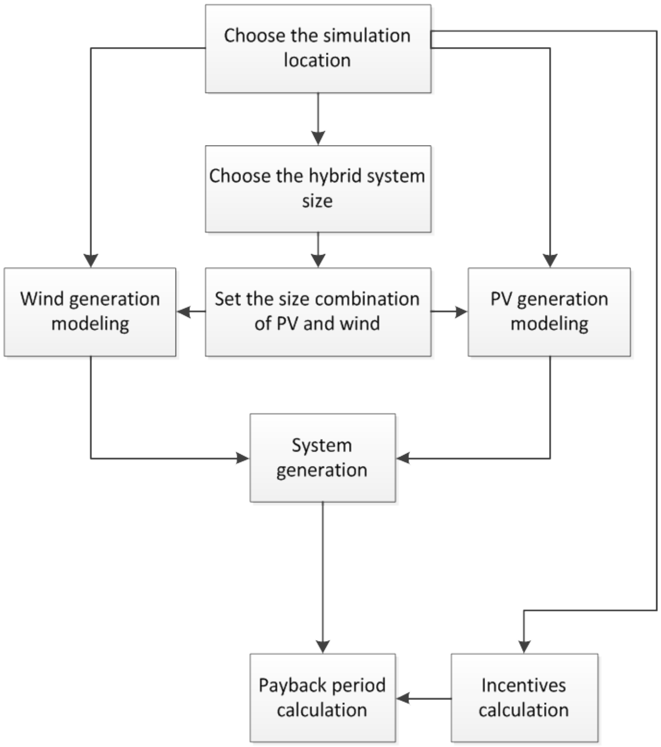

Figure 29 Process of payback analysis of the PV-wind hybrid system.

Assume a 4 kW hybrid system, and vary the PV panel size from 0 kW (no PV installed) to 4 kW (no wind turbines installed). Correspondingly, the wind turbine varies from 4 kW to 0 kW.

a) Wind generation

i) In Figure 30, we simulate a 4 kW wind turbine system. And the wind turbine output power value is arranged by the magnitude versus the hours. It indicates that the wind turbine generates power in 6596 hours of the entire year (8766 hours). The average is 1.44 kW, with a standard deviation is 0.93 and the median is 1.6 kW. That means in more than half of the time, it generates a power higher than 1.6 kW.

ii) While, in Figure 31, which shows the scenario for Midhill, we can see that the wind turbines only operates 3225 hours (nearly half of Altamont), and the output power mostly occurs on the interval of 1.2 to 1.4 kW. And the maximum output power is also nearly half of that in Altamont.

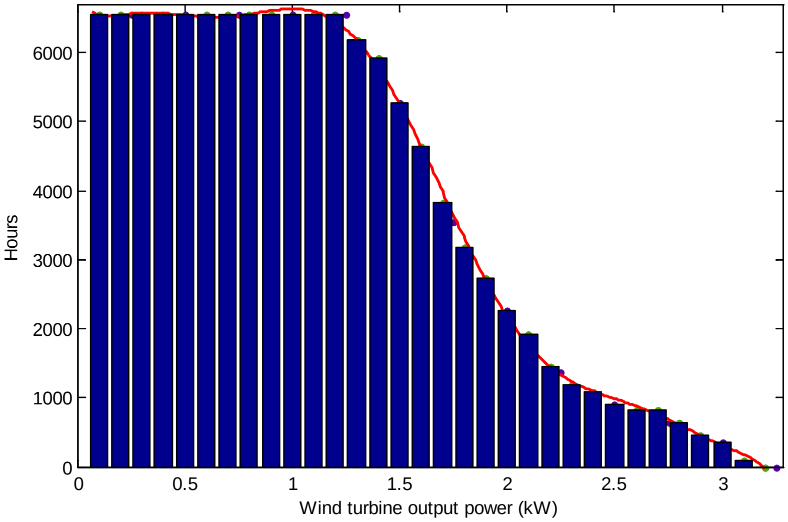

Figure 30 Cumulative probability distribution of wind turbine power output over one year in Altamont.

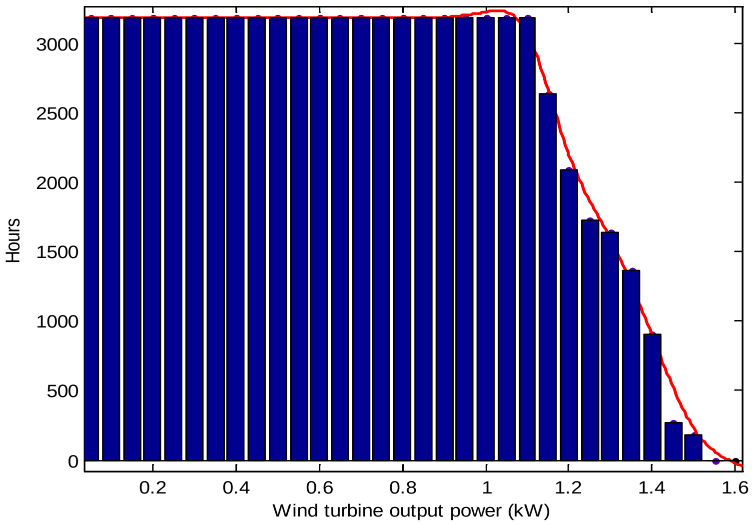

Figure 31 Cumulative probability distribution of wind turbine power output over one year in Midhill.

b) Solar generation

i) Figure 32 shows the annual output of a 4 kW solar PV system in Altamont. It was plotted in magnitude versus the total hours. The hourly average output power of the year is 0.72 kW, median is 0, and the standard deviation is 1.09. And for the daylight hours the average output power is 1.52 kW. Those data mean that during more than half a year, the PV does not generate power. And from the chart, we can see that the PV is expected to generate electricity during 3730 hours out of a year.

ii) Figure 33 shows the annual output in the Midhill scenario. Similarly, the operation time is around 3700 hours. This is because the operation time is generally decided by the daylight period, which has no significant difference between the two locations. However, the average output power in the daylight hours is 2.01 kW (0.49 kW larger than Altamont). Consequently, compared to the scenario in Altamont, Midhill is expected to produce more electricity with PV.

According to Figure 30 and Figure 32, wind turbines tend to operate more hours than PV in Altamont. Meanwhile, for a wind turbine and PV of the same size, the wind turbine is expected to generate more power than PV. However, in Midhill, PV panels and wind turbines have the similar functioning hours. And in contrast to Altamont, PV in Midhill seems to generate more power than the wind turbine.

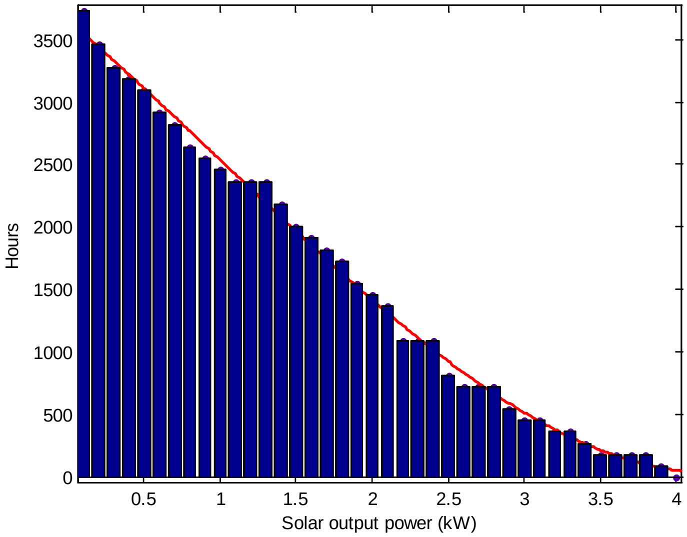

Figure 32 Cumulative probability distribution of PV power output over one year in Altamont.

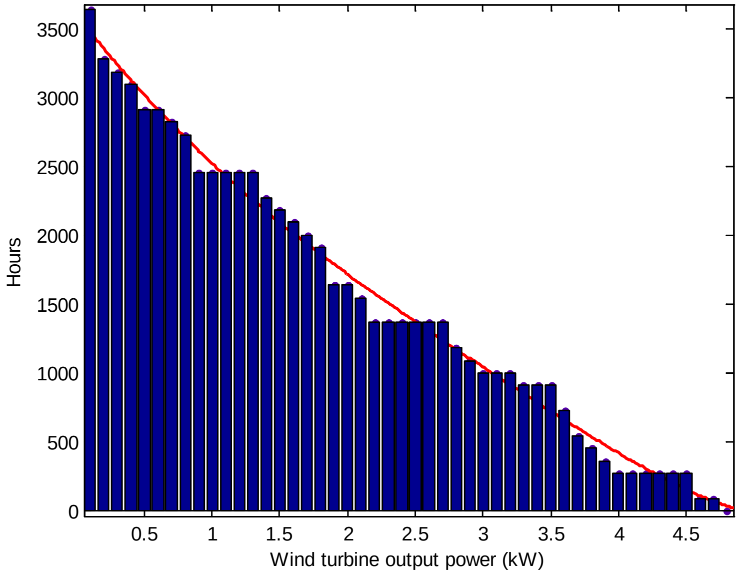

Figure 33 Cumulative probability distribution of PV power output over one year in Midhill.

c) PV-Wind with different size combinations

When combining the PV and wind turbines, the generation continues to vary depending on the size combinations.

Figure 34 and Figure 35 show the average energy generation of the hybrid solar and wind components of the hybrid system over different seasons, with different ranges of size combinations in both Altamont and Midhill.

For Altamont from the figure, we can see that the contribution of the solar and wind parts to the system energy output varies depending on the season and size. Clearly, in Altamont the contribution of PV generation is more significant than wind in winter. As referred to in Figure 26 and Figure 27, in winter, the wind speed rarely goes up to 3.5 m/s, which is the cut-in speed of the Skystream 3.7, while solar radiation still has an average around 0.3 kW/m^2. However, in general, both of them display larger generation in summer. And with the extraordinary wind resource, wind turbines perform a larger output proportion than that of PV through most of the year. Annually, under the same occupation of system size, PV contributes 31% of the total energy generation and wind turbines generate the remaining 69%.

On the other hand, in Midhill, obviously, the wind turbine plays a much less important role in the hybrid system. Compared with the wind performance in Altamont, wind generation in Midhill only made approximately 13% of the wind generation in Altamont based on the same wind turbine size. However, due to the consistent solar radiation level, the solar generation is 35% higher than that in Altamont. Above all, the solar generation makes 84% of the total generation in Midhill, while wind contributes only 16%.

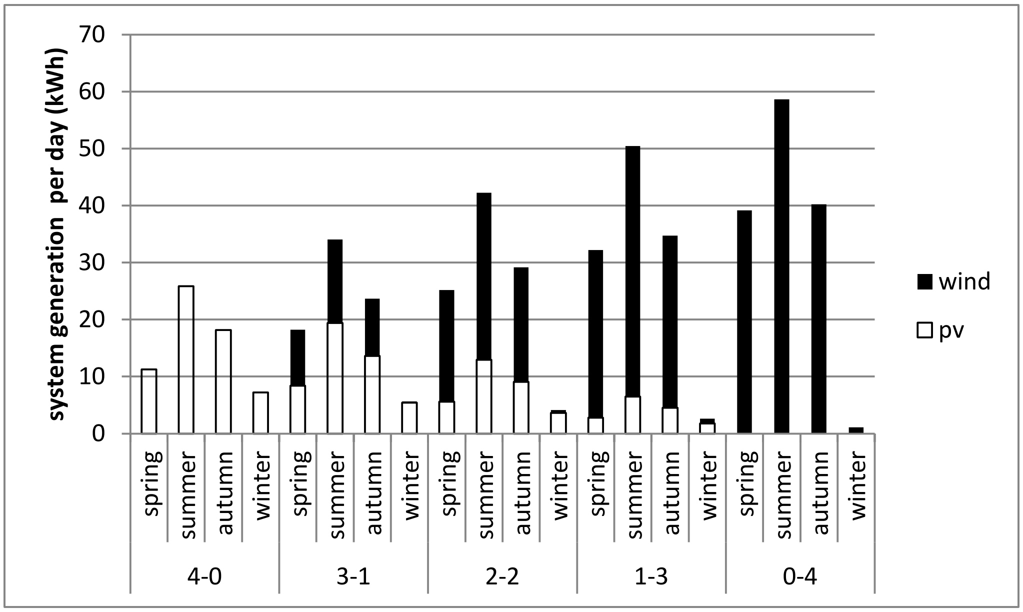

Figure 34 System generation per day with different size combinations in Altamont.

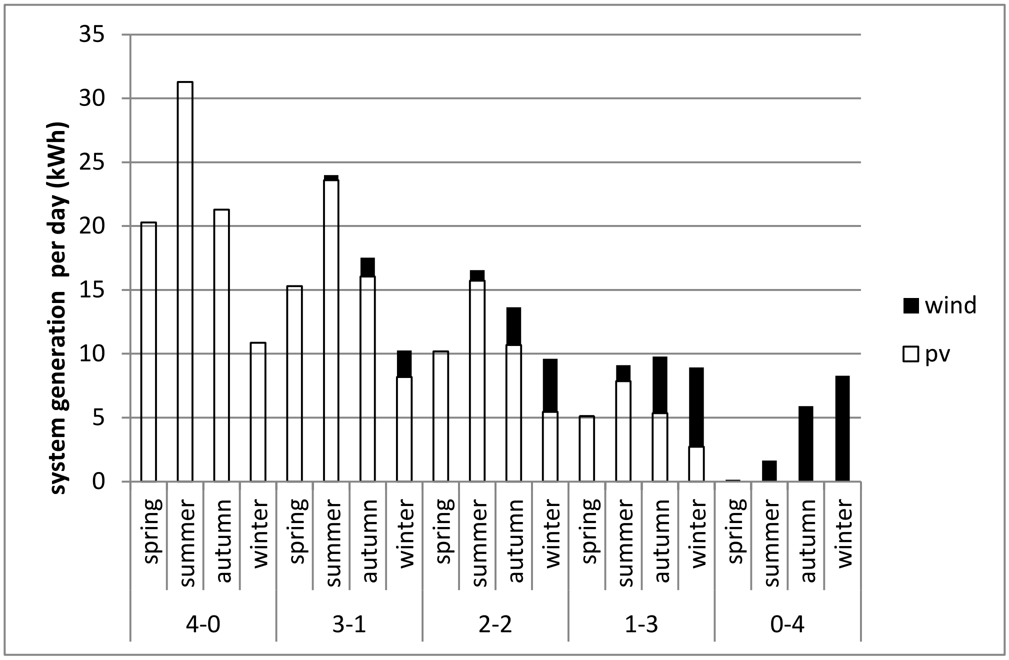

Figure 35 System generation per day with different size combinations in Midhill.

Table 21 shows the components of the hybrid system generation, and the specific contribution of each in the Altamont area. One can see that homeowners can increase the wind turbine size to obtain more hybrid generation.

Table 21: Altamont system generation with different size combination per year

Renewables type / PV-Wind Size Combination (kW)	**Solar**		**Wind**		**Hybrid Total** (kWh)
	Generation (kWh)	Proportion of whole system	Generation (kWh)	Proportion of whole system	
4-0	5682	100%	0	0%	5682
3-1	4262	57%	3164	43%	7426
2-2	2840	31%	6328	69%	9168
1-3	1419	13%	9492	87%	10912
0-4	0	0%	12656	100%	12656

4.1.3 Payback Analysis

We use the same method to calculate the payback conditions as in Sections 2.2 and 3.3. The equations are listed as Equations (7) – (8).

Here we assume all the PV panels are facing south. And the process to determine the payback period is shown as the flowchart in Figure 36.

Table 22 shows the results of the payback periods of Altamont and Midhill. Comparing the difference between the two locations, it can be seen that the payback period in Midhill decreases faster than that of Altamont as the PV size rises. For both locations, it takes less time to reach a breakeven point with a larger PV size.

Table 22: Payback period (years) of a hybrid system with two types of tariff under different system size combinations in California

		PV-Wind Size combination (kW)				
		0-4	1-3	2-2	3-1	4-0
Flat rate plan	Altamont	10.5	10.083	9.33	8.42	6.67
	Midhill	60.75	32.58	16.17	8.91	4.75
TOU plan	Altamont	10	9.17	8.17	6.67	4.83
	Midhill	27.08	16.58	10.58	6.67	3.83

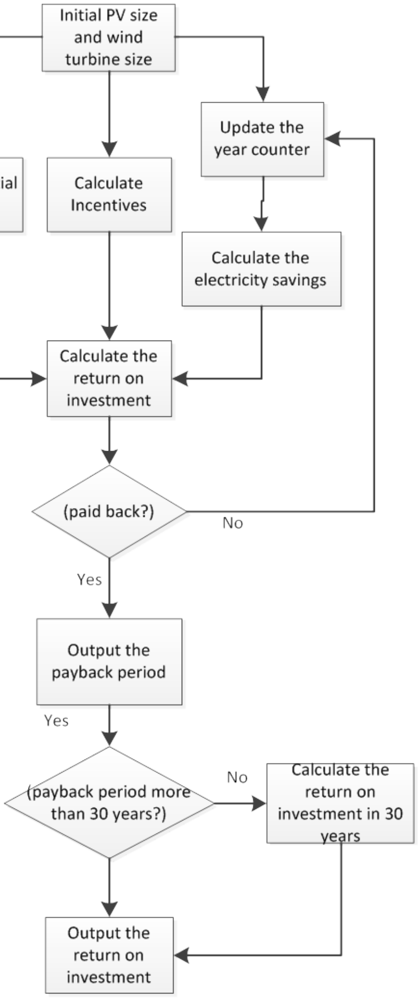

Figure 36 Process of calculating payback period.

(a)

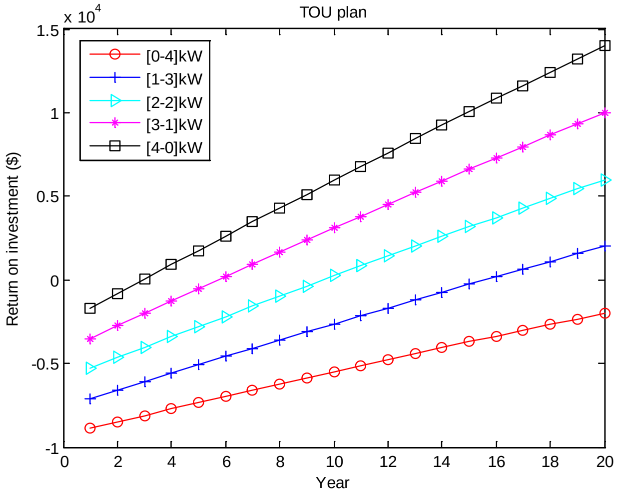
TOU plan
x 10^4
1.5
1
0.5
0
-0.5
-1
Return on investment ($)
0
2
4
6
8
10
12
14
16
18
20
Year
[0-4]kW
[1-3]kW
[2-2]kW
[3-1]kW
[4-0]kW

(b)

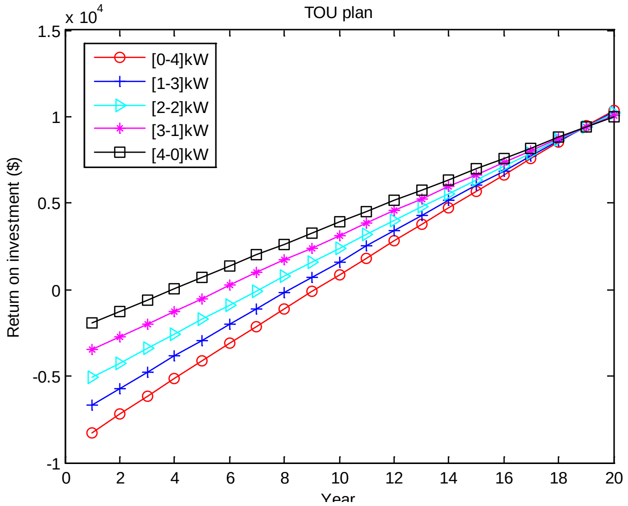
TOU plan
x 10^4
1.5
1
0.5
0
-0.5
-1
Return on investment ($)
0
2
4
6
8
10
12
14
16
18
20
Year
[0-4]kW
[1-3]kW
[2-2]kW
[3-1]kW
[4-0]kW

(c)

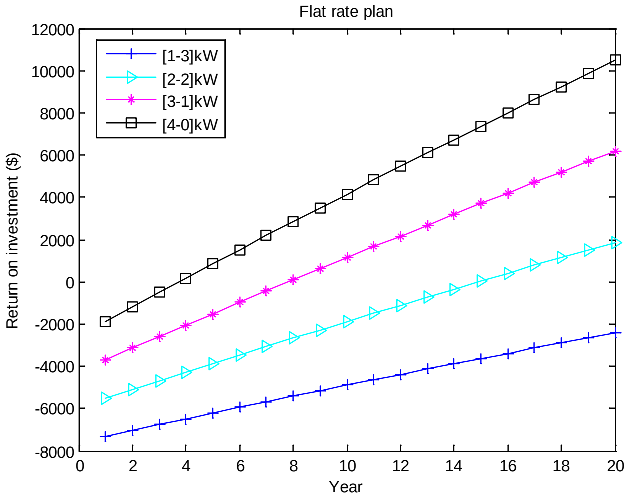
Flat rate plan
12000
10000
8000
6000
4000
2000
0
-2000
-4000
-6000
-8000
Return on investment ($)
0
2
4
6
8
10
12
14
16
18
20
Year
[1-3]kW
[2-2]kW
[3-1]kW
[4-0]kW

(d)

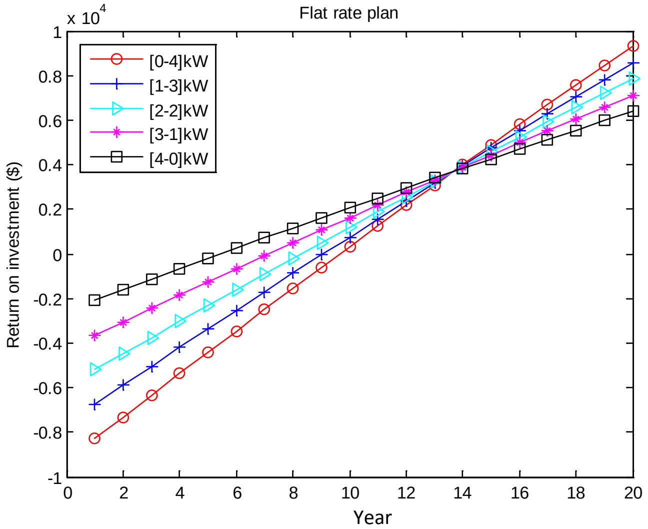

Figure 37 Return on investment with flat rate plan and TOU plan: (a) TOU plan in Midhill, (b) TOU plan in Altamont, (c) Flat rate plan in Midhill, (d) Flat rate plan in Altamont.

Figure 37 shows the return on investment based on two different tariffs in both Altamont and Midhill. PV has a lower cost around $ 3.4/W, while for a wind turbine it cost $6.3/W. As a consequence, the initial remaining investment for PV is much lower than the wind turbines. However, since wind turbines function in a more productive way than that of PV, the more the wind generation that is put into the hybrid system, the more the electrical savings would be and the investment curve would go up faster and steeper. After 14 years for the flat rate plan (19 years for TOU plan), the return on investment reaches the same value. Then after that, the bigger the wind turbine size is, the more the return we can gain. Although it is faster to reach a breakeven point with a larger PV, the return on investment is expected to increase slower.

Despite this, in Midhill, the larger wind turbine always means a higher initial cost and less yearly investment return. From Figure 37, we can see the larger the PV size, the steeper the curve is, that means a faster return rate on the investment. This is a consequence of weak wind resource which leads to less electricity generation and less electrical savings.

We can see that, even though we suppose Altamont and Midhill are under the same incentives condition, the energy resource still makes a big difference on the economic performance.

4.2 Real Case

As the real life case, certain wind turbines and PV panels are chosen to examine the system performance in Midhill and Altamont. Here we choose the wind turbine Skystream 3.7, as mentioned previously, the rated size is 2.4 kW, and we choose the Suntech PV panels with size of 2 kW.

4.2.1 Fixed generation and variable incentives

As we know, as the renewable energy is more and more acknowledged by the public, the renewable generation capacity goes up gradually. And when the penetration of the renewables reaches a higher proportion, the incentives tend to be reduced. Moreover, impacts of high penetration of renewables on the transmission and distribution system also may lead to a higher cost for the utility.

On the other hand, most incentive programs are expiring before 2020. A predictable trend of declining incentives will emerge by then. Besides, throughout the U.S., the incentives vary from state to state. Like we mentioned before in AZ, the utility rebate for the PV is only \$0.6/W while in California, it is \$2.5/W. Thus analysis of the impacts of incentives on the hybrid system economic performance is necessary.

For California, the state incentive (Buy-down program) now is \$3/W for the wind turbines and \$2.5/W for PV. Under these circumstances, the payback period can be calculated, which is 11.33 years (11 years and 4 months) with the TOU plan for a 4 kW system.

Now, we vary the incentives (utility rebate) of both wind turbines and PV from \$0.5/W to \$3/W. With the algorithm presented in the previous section, we have the result of payback periods as shown in Table 23.

Table 23: Payback period (years) of a hybrid system with two tariff types under different utility rebates in California

Tariff Type	**Utility Rebate ($/W)**					
	0.5	1	1.5	2	2.5	3
TOU plan	22.83	20.25	17.67	15.17	12.67	10.25
Flat rate plan	37.42	32.75	28.33	24	19.833	15.83

The return on investment is plotted in Figure 38. Observing the table and figures, it can be seen that higher incentives lead to shorter payback periods by around 5 years/$ for the TOU plan and 9 years/$ for the flat rate plan.

Thus we define the sensibility of utility rebate incentives as,

$$S_1 = \frac{[length(0.5) - length(3)]year}{(3-0.5)\$} \approx \begin{cases} 5year\,/\,\$/\mathrm{W} & \text{(TOU)} \\ 9year\,/\,\$\,/\,\mathrm{W} & \text{(Flat\_rate)} \end{cases} \tag{20}$$

(a)

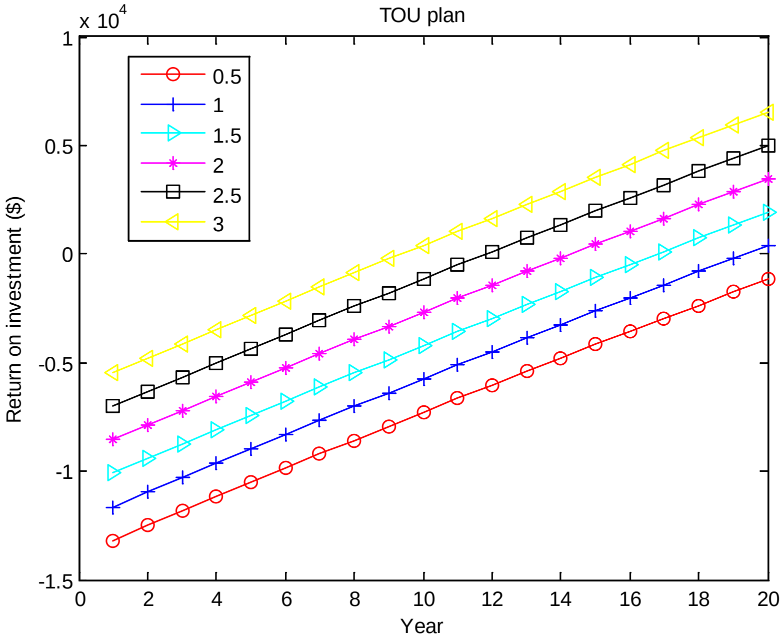

(b)

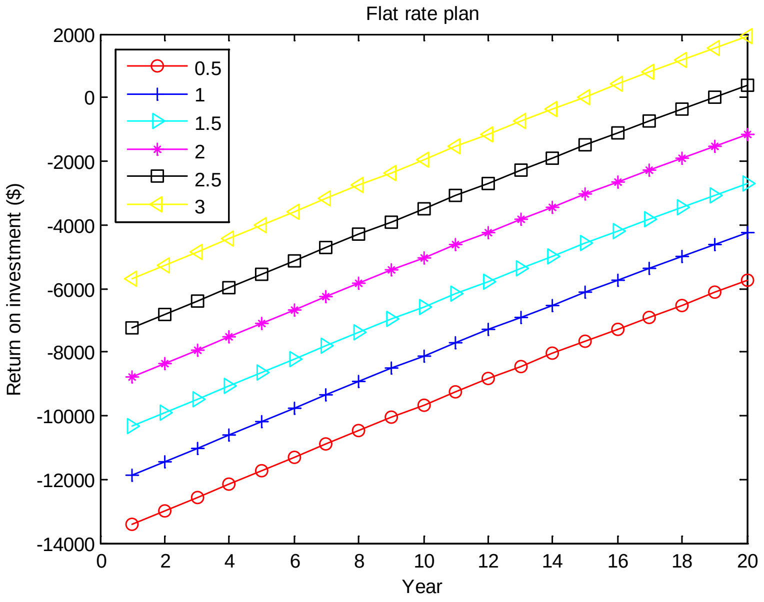

Figure 38 The payback period (year) with different system rebate under (a) TOU plan, (b) flat rate plan.

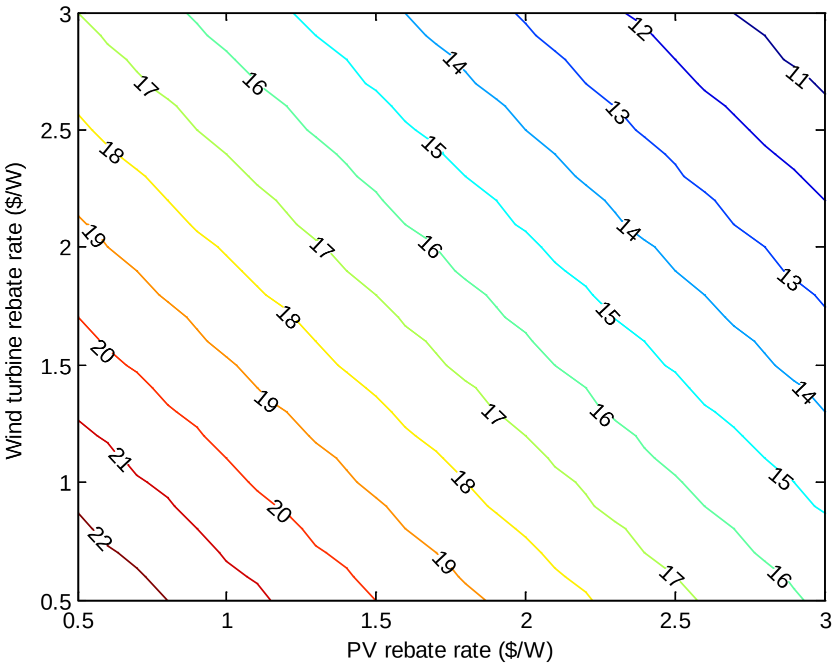

Figure 39 The payback period (year) for any PV rebated rate with respect to wind turbine rebate rate with TOU plan.

Figure 39 shows the payback condition with the PV and wind turbine rebate rate ranging from \$0.5/W to \$3.0/W. The hybrid system with higher rebate rate therefore achieves a shorter payback period than the one with lower rebate rate.

From the DISRE website, it can be concluded that most of the states have wind rebates in the range from \$1/W to \$2.5/W, and PV is around \$1/W to \$2/W. Under the same conditions as Midhill, the payback period is around 22 years to 14 years.

4.2.2 PV and Wind Turbine Cost

From Chapter 2, it can be observed that the PV panel price is reducing year by year. Since 2000, it has declined from \$10/W to around \$4/W in 2010 and expects to continue reducing in the future. Similarly, the wind turbines have a much lower cost in recent years than that 10 years ago, although it fluctuates in recent years. To research the impact of different PV and wind turbine cost on the economic performance of the hybrid system, we arrange the PV cost ranging from \$1/W to \$8/W while wind turbine cost ranging from \$3/W to \$10/W.

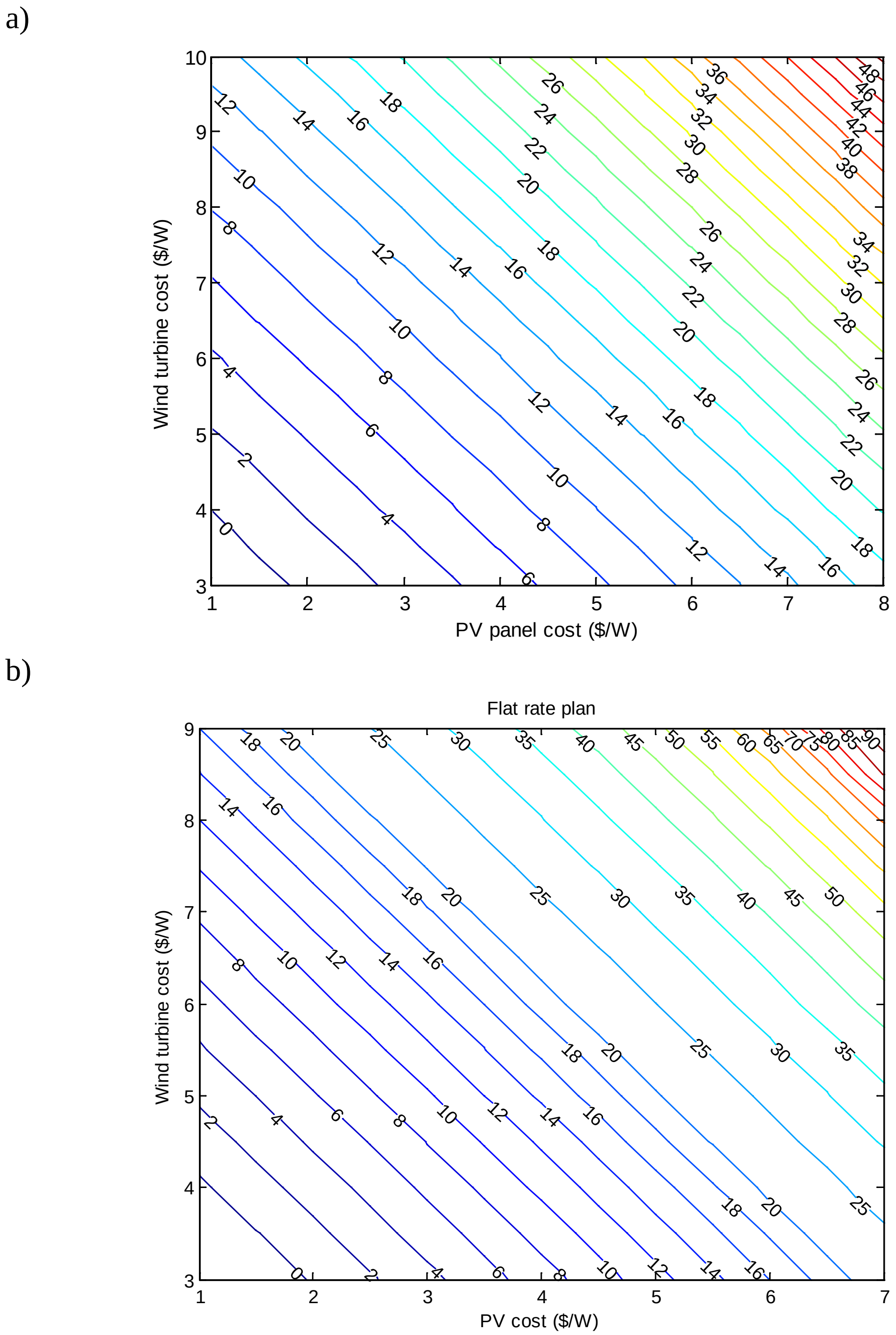

Figure 40 The payback period with different wind turbine costs and PV panel costs: (a) TOU plan, (b) Flat rate plan.

From the figure, it can be indicated that higher PV and wind turbine cost lead to longer payback period. The curves in Figure 40 tends to be more dense as the cost increase; that means the higher the cost is, the faster the payback period increases.

Also, we can get from the Figure 40 that, to achieve a payback period less than 10 years, the wind and PV cost should satisfy following requirements:

$$C_{wind} + 1.51 C_{PV} < 8.82 \qquad (C_{PV} < 5.85, C_{wind} < 8.82) \qquad \text{(TOU plan)} \qquad (21)$$

$$C_{wind} + 1.58 C_{pv} < 7.45 \qquad (C_{pv} < 4.73, C_{wind} < 7.45) \qquad \text{(Flat rate plan)} \ (22)$$

Where,

C_{wind}: the cost of wind turbines ($/W);

C_{PV}: the cost of PV panels ($/W).

Then we do some research on the condition that PV cost takes the values from $1/W to $8/W, while the wind turbine cost varies from $3/W to $10/W. The calculations are performed only for the situation in which wind turbine cost is $2 more than PV.

Accordingly, the system cost can be obtained as,

$$C = (2000 C_{PV} + 2400 C_{wind}) / 4400 \qquad (23)$$

And the payback period is calculated and plotted as Figure 41. Then using the MATLAB curve fitting tool, we can determine the approximate function of the payback period with respect to the system cost,

$$Year = 0.09948C^3 - 0.918C^2 + 7.126C - 13.79 \tag{24}$$

Year: the payback period (year).

Thus we can get the slope of the function is,

$$S_2 = 0.298C^2 - 1.836C + 7.126 \tag{25}$$

The slope can show the impact of the system cost change on the payback period. Hence, we define the slope S_2 as the *sensibility of system cost*. Table 22 shows the S_2 values with a range of system cost. Clearly, as the system cost goes up, the payback period tends to be more sensible. The system cost has a more significant effect on the payback period.

Table 24: The sensibility of cost with respect to the system cost

System Cost	2	3	4	5	6	7	8	9	10
S_2 (year/$/W)	4.6	4.3	4.6	5.4	6.8	8.9	11.5	14.7	18.6

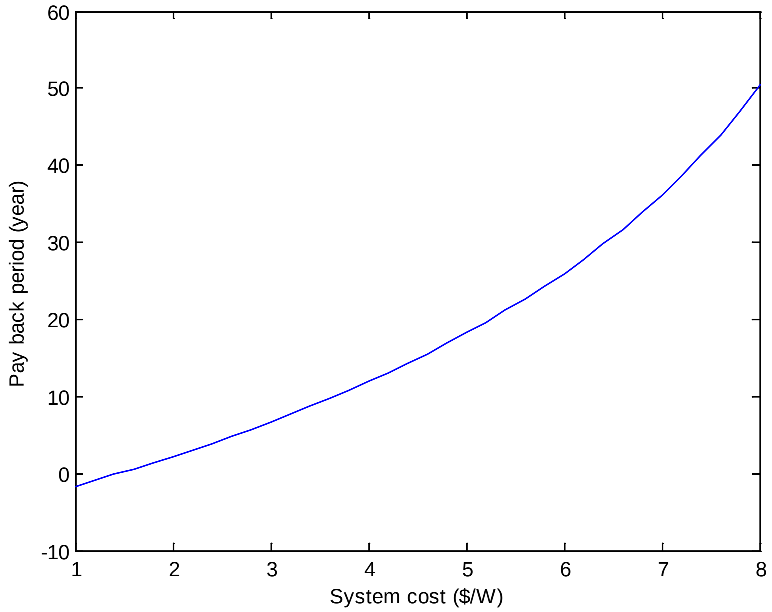

Figure 41 The payback period with respect to the system cost.

4.2.3 Comparison

We obtained the sensibility of the incentives and the system cost. As the system cost is around $5/W recently, the sensibility for TOU plan is around 5 year/$/W to 6 year/$/W accordingly from Table 22. Meanwhile, the sensibility of the incentives also has a similar value of 5 year/$/W.

5. CONCLUSION

Within this thesis, the economic performance of the residential renewable energy system is analyzed. PV and wind power are first evaluated separately, then a hybrid system is assessed. Factors of environmental parameters and also marketing elements are included.

1. Solar

PV is affected by the irradiance level and the incentives, and also the orientations and tilt angles of the panel. In Chapter 2, we assume a 4 kW PV system in Arizona served by APS, and the analysis of the economic performance of the system is based on different orientations, which lead to different incident radiation. As buildings in Arizona are mostly built with a roof angle of 18.01°, we fixed the panels with that angle, and set the orientations as east, southeast, south, southwest, and west.

Clearly, it is found that in northern hemisphere, we can obtain the most radiation with a panel facing south; and then followed by southwest, southeast, west and east. Generally, PV panels facing westward tend to generate more power than those facing eastward. However, in contrast with the flat rate plan, with the TOU plan, the most generation does not equal the most electricity savings. Since the electricity rate reaches a higher level during the peak time in the afternoon, which makes the electricity generated then more valuable. Consequently, PV towards southwest which is more productive in the afternoon achieves the most electricity savings. Therefore, it also means a shorter payback period.

(*Note: For southern hemisphere, the ‘south’ needs to be converted to ‘north’, ‘southwest’ to ‘northwest, ‘southeast’ to ‘northeast’ accordingly.)

2. Wind Power

Wind power is an intermittent energy resource, and significantly affected by the geographic factors. Even in two very close locations, wind resources can be very different. In Chapter 4, we research the wind turbine performance within two different locations, California and Arizona, which have quite different wind resources and incentive systems.

Software is developed to test the payback period with a range of wind speed corresponding to the location. The Skystream 3.7 wind turbine is chosen as a certified grid-tied small wind turbine to apply in the system. The results show that higher wind speed leads to a better economic performance. Specifically, in Arizona, if the wind speed increases from 5 m/s to 13 m/s, the payback period is reduced by 9 years; while in California, the reduction is 30 years. In addition, incentives and net metering price have impacts on the payback period as well. Better incentives and net metering contribute to a shorter payback period, which can be observed from the difference between the Arizona case and the California cases.

3. PV-Wind Hybrid system

In Chapter 4, the impacts of each component on a hybrid system are analyzed. First of all, the different size combinations lead to different energy output and also different incentive structure. Meanwhile, it has a regional difference as well. Thus two specific locations (Midhill and Altamont, CA) are selected accordingly to include the regional factors. Thus we can see that, although a system with larger PV always has a shorter payback period due to the lower base cost, for places with better wind resources than solar, after a certain year, larger wind turbines lead to a higher return on investment. Furthermore, the impacts of incentives for both renewables are researched. As expected, the result shows that the hybrid system with a higher rebate rate therefore achieves a shorter payback period than the one with a lower rebate rate. On the other hand, the impact of installing base cost of both renewables is discussed. Also as expected, higher PV and wind turbine costs lead both to longer payback periods, while the payback period tends to have a steeper slope as the cost increases; that means the higher the cost is, the faster the payback period increases.

4. Future work

There are still many potential works that may be included in the future.

1) Incentives like 3rd party programs are not included in the thesis. Third party programs allow people to have a third party install a renewable system in one's own home, while the installer receives the incentives such as, cash rebate, tax credit and so on, whereas the homeowner would achieve a lower electricity price by interconnecting the system to the grid. This is also a promising way to get renewable systems at home. However, the payback with a third party is more complicated as it involved in more than one benefiter, and more complicated cost calculation.
2) Also other factors, such as the increase of the electricity prices, the money value changes caused by the inflation, the price of the equipment material and so on, also impact the economic performance of renewable systems continuously.
3) For the wind turbine, we chose only the Skystream during the research. We chose it because there are only three small grid-tied wind turbines that have

been certified by the SWCC. By the requirements of most states, a certified wind turbine is necessary to get the system approved. However, more and more certified wind turbines and new manufacturer s may emerge in the near future.

4) With residential-sized system, we assume the system around 4 kW, while actually, system can be up to 10 kW, like for some farms.
5) Moreover, the relationship between the time variation of generation and the load are not discussed in the thesis.

REFERENCES

[1] NREL open PV project. (2012, Jul. 18). NREL, Golden, Colorado. [Online]. Available: http://openpv.nrel.gov

[2] Ryan Wiser, Mark Bolinger, “2008 Wind technologies market report,” NREL, Golden, Colorado, Contract No. DE-AC36-08-GO28308, Jul. 2009.

[3] Wind generation map. (2012, Jul. 18). U.S. Department of Energy. Washington D.C. [Online]. Available: http://www1.eere.energy.gov/wind/

[4] Renewables 2011: Global Status Report. REN21. (2012, Jul. 18). [Online]. Available: www.ren21.net

[5] Salameh Z.M., Borowy B.S., Amin, A.R.A., "Photovoltaic module-site matching based on the capacity factors, "*IEEE Transactions on Energy Conversion*, vol. 10, no. 2, pp. 326-332, Jun 1995.

[6] Jinhuan Yang, Liang Ge and Peiyue Tan, Zhonghua Chen, Qianlin Zou, "Application of photovoltaic system," in *Shanghai Power*, Shanghai, China: Shanghai Power College. 2006, pp. 356-361.

[7] Paul Denholm, Robert M. Margolis, Sean Ong and Billy Roberts, “Break-even cost for residential photovoltaics in the United States: key drivers and sensitivities,” NREL, Golden, Colorado, Tech. Rep.TP-6A2-46909, Dec. 2009.

[8] Jason Coughlin and Karlynn Cory, “Solar photovoltaic financing: residential sector deployment,” NREL, Golden, Colorado, Tech. Rep. TP-6A2-44853, Mar. 2009.

[9] Ben Hoen, Ryan Wiser, Peter Cappers and Mark Thayer, “An analysis of the effects of residential photovoltaic energy systems on home sales prices in California,” LBNL, Berkeley, CA, Rep. LBNL-4476E, Apr. 2011.

[10] T.Forsyth, P. Tu, and J. Gilbert, “Economics of grid-connected small wind turbines in the domestic market,” NREL, Golden, Colorado, Contract DE-AC36-99GO10337, June 20-23, 1999.

[11] Zeng Ming, Sikaer, A., Geng Weiting, Li Chen, "Economic Analysis of the Stability in the Wind Turbine Selection," *Power and Energy Engineering Conference (APPEEC)*, pp. 1-4, March 28-31, 2010.

[12] Jain, A. M. and Kushare, B. E., "Techno-economics of solar wind hybrid system in Indian context: A case study," *IET-UK International Conference on ICTES*, Dec. 20-22, 2007, pp. 39-44.

[13] Soysal, O.A. and Soysal, H.S., "A residential example of hybrid wind-solar energy system: WISE," *Power and Energy Society General Meeting - Conversion and Delivery of Electrical Energy in the 21st Century, 2008 IEEE* , pp. 1-5, July 20-24, 2008.

[14] A. Driesse, S. Harrison, and P. Jain, "Evaluating the effectiveness of maximum power point tracking methods in photovoltaic power systems using array performance models," *Proc. IEEE Power Electron. Spec.Conf.*, 2007, pp. 145–151.

[15] *NFPA 70: National electrical code®*, NEC. CA, 2011.

[16] G. Lewis, "Optimum tilt of a solar collector," *Solar & Wind Technology*, 1987. vol. 4, pp. 407-410.

[17] H. M. S. Hussein, GE Ahamd, H.H. El-Ghetany, "Performance evaluation of photovoltaic modules at different tilt angles and orientations," *Energy Conversion and Management*, 2004, vol. 45, pp. 2441-2452.

[18] D. Ibrahim, "Optimum tilt angle for solar collectors used in Cyprus," *Renewable energy*, 1995, vol. 6, pp. 813-19.

[19] Hiller, W. Amft, D. and Ebest, G., "Optimization of the PV-yield in solar facades by different directions," *Photovoltaic Specialists Conference*, Sep-Oct. 1997, pp. 1337-1340.

[20] Akhmad K, Belley F, Kitamura A, Yamamoto F and Akita S., "Effect of installation conditions on the output characteristics of photovoltaic modules," *IEEE photovoltaic specialists conference*, Hawaii, 1994, pp. 730–3.

[21] J. Mondol, Y. Yohanis, and B Norton, "The impact of array inclination and orientation on the performance of a grid-connected photovoltaic system," *Renewable Energy*, 2007, vol. 32, pp. 118-140.

[22] Bari S., "Optimum slope angle and orientation of solar collectors for different periods of possible utilization," *Energy Conversion and Management*, 2000, vol. 41, pp. 855-860.

[23] Keith E. Holbert and Devarajan Srinivasan, "Chapter 8: Solar Energy Calculations," in *Handbook of Renewable Energy Technology*, 1st ed. Hackensack, NJ: World Scientific, 2011, pp. 188-204.

[24] Daniel Walsh, “Connecting your Wind Generator to the Grid,” *Renewable Energy*, pp. 436-466, 2001.

[25] 2010 U.S. Small Wind Turbine Market Report. (2012, Jul.18). AWEA, Washington, DC. [Online]. Available: www.awea.org

[26] Small Wind Turbine Performance and Safety Standard., (2012, Jul.18). AWEA, Washington, DC. [Online]. Available: http://www.awea.org/learnabout/smallwind/upload/AWEA_Small_Turbine_Standard_Adopted_Dec09.pdf

[27] *Skystream 3.7 brochure*. (2012, Jul.18). Southwest Windpower Corp. Flagstaff, AZ. [Online]. Available: http://www.windenergy.com/products/skystream/skystream-3.7

[28] *Excel 10 brochure*. (2012, Jul.18). Bergey WindPower Co. Norman, OK. [Online]. Available: http://www.bergey.com/products/wind-turbines/10kw-bergey-excel

[29] Y. Gao R. Billinton, “Adequacy assessment of generating systems containing wind power considering wind speed correlation”, *IET Renew. Power Gener.*, 2009, vol. 3, pp. 217 – 226.

[30] Giorsetto P., Utsurogi K.F., “Development of a new procedure for reliability modeling of wind turbine generators,” *IEEE Trans. Power Appar. Syst.*, 1983, vol. PAS-102, no. 1, pp. 134-143.

[31] APS - Renewable Energy Incentive Program. (2012, Jul.18). Arizona Public Service Co. Phoenix, AZ. [Online]. Available: http://www.dsireusa.org/incentives/incentive.cfm?Incentive_Code=AZ04F&re=1&ee=1

[32] Edmund G. Brown, Jr., Governor. (Nov. 2011). Emerging renewables program guidebook. [Online] Available: http://www.energy.ca.gov/2011publications/CEC-300-2011-004/CEC-300-2011-004-ED12-CMF.pdf

[33] Public Utilities Commission. (2008). *Net Energy Metering Standard*. [Online]. Available: http://www.cpuc.ca.gov/PUC/energy/DistGen/netmetering.htm

[34] PV Solar Radiation Static Maps. (2012, Jul.18). NREL, Golden, Colorado. [Online]. Available: http://openpv.nrel.gov

[35] Wind rose of central CA. (2012, Jul.18). The Western Regional Climate Center, NV. [Online]. Avaible: http://www.wrcc.dri.edu/

[36] R. Chedid and Saifur Rahman, "A decision support technique for the design of hybrid solar-wind power systems", *IEEE Trans. on Energy Conversion*, March 1998,Vol. 13, No. 1, pp. 76-83.

[37] Hiraoka S, Fujii T, Takakura H and Hamakawa Y., "Tilt angle dependence of output power in an 80kWp hybrid PV system installed at Shiga in Japan," *Sol Energy Mater Sol Cells*, 2003, vol. 75, pp. 781-786.

[38] Soysal O.A. and Soysal H.S., "A residential example of hybrid wind-solar energy system: WISE," *Power and Energy Society General Meeting*, July 2008, pp. 1-5, 20-24.

[39] Jayanta Deb Mondol, Yigzaw G. Yohanis and Brian Norton, "The impact of array inclination and orientation on the performance of a grid-connected photovoltaic system," *Renewable Energy*, January 2007, vol. 32, pp. 118-140.

[40] Ibrahim Reda and Afshin Andreas, "Solar Position Algorithm for Solar Radiation Applications," National Renewable Energy Laboratory, Jan. 2008.

[41] Akhmad K., Belley F., Kitamura A., Yamamoto F., Akita S., Takakura, H., et al., "Effect of installation conditions on the output characteristics of photovoltaic modules," *IEEE Photovoltaic Specialists Conference*, Dec. 1994, vol. 1, pp. 730-733.

[42] Alonso-Garcia M.C., Ruiz J.M. and Herrmann W., "Computer simulation of shading effects in photovoltaic arrays," *Renew Energy*, 2006, vol. 31, no. 12, pp. 1986-1993.

[43] S. Chowdhury, G. A. Taylor, S. P. Chowdhury, A. K. Saha, and Y. H. Song, "Modeling, simulation and performance analysis of a PV array in an embedded environment," *Proc. 42nd Int. Univ. Power Eng. Conf.*, 2007, pp. 781-785.

[44] Gao, Y. and Billinton, R., "Adequacy assessment of generating systems containing wind power considering wind speed correlation," *Renewable Power Generation, IET*, vol. 3, no. 2, pp. 217-226, Jun. 2009.

[45] Crispim Joao, Carreira Micael and Castro Rui, "Validation of Photovoltaic Electrical Models against Manufacturers Data and Experimental Results," *International Conference on POWERENG 2007*, Apr. 2007, pp.556-561.

[46] Balouktsis A., Tsanakas D., Vachtsevanos G., “On the optimum tilt angle of a photovoltaic array,” *Int. J. Solar Energy*, vol. 5, no. 3, 1987, pp. 153-169.

[47] P. M. Anderson and A. Bose, “Stability simulation of wind turbine systems,” *Power App. Syst.*, Dec. 1983, vol. 102, pp. 3791–3795.

[48] El-Tamaly, H.H. and Mohammed, A.A.E., "Modeling and simulation of Photovoltaic/Wind Hybrid Electric Power System Interconnected with electrical utility," *Power System Conference. 12th International Middle-East,* March 2008, pp. 645-649.